Matematisk-fysiske Skrifter
udgivet af
Det Kongelige Danske Videnskabernes Selskab
Bind **3**, nr. 1

Mat. Fys. Skr. Dan. Vid. Selsk. **3**, no. 1 (1965)

THE RESTRICTED PROBLEM OF THREE BODIES (II)

BY

J. H. BARTLETT AND C. A. WAGNER

København 1965
Kommissionær: Ejnar Munksgaard

DET KONGELIGE DANSKE VIDENSKABERNES SELSKAB udgiver følgende publikationsrækker:

THE ROYAL DANISH ACADEMY OF SCIENCES AND LETTERS *issues the following series of publications:*

	Bibliographical Abbreviation
Oversigt over Selskabets Virksomhed (8°) *(Annual in Danish)*	Overs. Dan. Vid. Selsk.
Historisk-filosofiske Meddelelser (8°)	Hist. Filos. Medd. Dan. Vid. Selsk.
Historisk-filosofiske Skrifter (4°) *(History, Philology, Philosophy, Archeology, Art History)*	Hist. Filos. Skr. Dan. Vid. Selsk.
Matematisk-fysiske Meddelelser (8°)	Mat. Fys. Medd. Dan. Vid. Selsk.
Matematisk-fysiske Skrifter (4°) *(Mathematics, Physics, Chemistry, Astronomy, Geology)*	Mat. Fys. Skr. Dan. Vid. Selsk.
Biologiske Meddelelser (8°)	Biol. Medd. Dan. Vid. Selsk.
Biologiske Skrifter (4°) *(Botany, Zoology, General Biology)*	Biol. Skr. Dan. Vid. Selsk.

Selskabets sekretariat og postadresse: Dantes Plads 5, København V.

The address of the secretariate of the Academy is:

Det Kongelige Danske Videnskabernes Selskab,
Dantes Plads 5, København V, Denmark.

Selskabets kommissionær: EJNAR MUNKSGAARD's Forlag, Nørregade 6.
København K.

The publications are sold by the agent of the Academy:

EJNAR MUNKSGAARD, *Publishers,*
6 Nørregade, København K, Denmark.

Matematisk-fysiske Skrifter
udgivet af
Det Kongelige Danske Videnskabernes Selskab
Bind **3**, nr. 1

Mat. Fys. Skr. Dan. Vid. Selsk. **3**, no. 1 (1965)

THE RESTRICTED PROBLEM OF THREE BODIES (II)

BY

J. H. BARTLETT AND C. A. WAGNER

København 1965
Kommissionær: Ejnar Munksgaard

Synopsis

Periodic solutions have been found for the motion of a sputnik in the gravitational field of two other bodies of finite mass. The simple symmetric classes (a), (f), and (n) have been studied for the full mass-ratio range $-1 \leq \gamma \leq 1$, and classes (β), (δ), ($\alpha - \delta$), and ($g - f$) for the range $-1 \leq \gamma \leq 0.93$.

When the mass-ratio γ changes, separate parts of an eigensurface may approach each other, touch, and split apart in another mode. (More complicated interactions with the zero-velocity surfaces also occur.) When a branch of a class terminates on an asymptotic orbit, and a companion branch on the conjugate asymptotic orbit, then the two branches will join when these asymptotic orbits coalesce. This happens for the (g) class: at $\gamma = 0$ one branch terminates on asymptotic orbits VII and VIII, but at $\gamma = -9/11$ the class has been transformed into a larger ($g - f$) class which apparently does not terminate.

PRINTED IN DENMARK
BIANCO LUNOS BOGTRYKKERI A/S

In a previous communication[1], a systematic study has been made of simple classes of periodic solutions which are present when a sputnik is moving under the gravitational action of two other bodies of equal finite mass. The present article extends the treatment to the case where the finite bodies have any mass ratio from zero to infinity. Shearing[2] made some computations for the ratio of one to ten, but did not use the Thiele[3] system of coordinates and so could not run any class past a collision orbit. We have remedied this situation, and include the results of Shearing in our tables. Since the main purpose of our work is to demonstrate the overall topological structure of the restricted three-body problem and how the classes appear, evolve and disappear, extreme precision of calculation has not been attempted.

Equations of Motion

Two bodies S and J, with masses m_1 and m_2 respectively, execute circular motions about their common center of gravity, which lies at the origin. A third body P with vanishing small mass moves in the same plane as m_1 and m_2 do. The distances between these points are $SJ = 2$, $SO = r_1$, $OJ = r_2$, $SP = r$, and $PJ = \varrho$. In the rotating coordinate system (ξ, η), the ξ-axis lies along the direction SJ, and the angular velocity $\omega = 1$.

The equations of motion are then

$$\ddot{\xi} - 2\dot{\eta} = \partial U/\partial \xi \quad \text{and} \quad \ddot{\eta} + 2\dot{\xi} = \partial U/\partial \eta \tag{1}$$

where

$$2U = \xi^2 + \eta^2 + 8(1+\gamma)/r + 8(1-\gamma)/\varrho \tag{2}$$

and

$$\gamma = (m_1 - m_2)/(m_1 + m_2).$$

The first integral of (1) is

$$\dot{\xi}^2 + \dot{\eta}^2 = 2U - K \tag{3}$$

where K is the Jacobi constant.

1*

The THIELE transformation to regularize the solutions is

$$\left.\begin{aligned} \xi &= ch\,F\cos E + \gamma \\ \eta &= -sh\,F\sin E \\ d\psi &= dt/r\varrho = dt/D \\ \text{where}\quad 2D &= ch\,2F - \cos 2E. \end{aligned}\right\} \tag{4}$$

Using a dot in what follows to denote differentiation *re* ψ rather than *re* t, we have

$$\left.\begin{aligned} \frac{2H}{D} \equiv \frac{\dot E^2 + \dot F^2}{D} = -\frac{T}{2} + \frac{8}{D}(ch\,F - \gamma\cos E) + \frac{1}{4}(ch\,2F + \cos 2E) \\ + \gamma\, ch\,F\cos E = -(K/2) + U \end{aligned}\right\} \tag{5}$$

where $T = K - \gamma^2$.
Also,

$$\left.\begin{aligned} \ddot E = 2D\dot F + (1/4)\sin 4E - (T/2)\sin 2E \\ -(\gamma/4)(\sin E\, ch\,3F - 3\sin 3E\, ch\,F - 32\sin E) \end{aligned}\right\} \tag{6}$$

and

$$\left.\begin{aligned} \ddot F = -2D\dot E + (1/4)\,sh\,4F - (T/2)\,sh\,2F + 8\,shF \\ -(\gamma/4)(-3\cos E\, sh\,3F + \cos 3E\, shF). \end{aligned}\right\} \tag{7}$$

These equations are invariant under the transformation

$$E' = E + \pi,\ F' = F,\ \gamma' = -\gamma. \tag{8}$$

Accordingly, the set of $(T,\ E)$ profiles for $0 \le E \le \pi$ and $-1 \le \gamma \le 1$ will be equivalent to that for $0 \le E \le 2\pi$ and $-1 \le \gamma \le 0$. This transformation amounts to interchanging the masses and replacing ξ, η by $-\xi$, $-\eta$, from which it is apparent that the equations will remain the same. Equations (6) and (7) are also invariant under the transformation $F' = -F$, $E' = E$, $t' = -t$, so that the motion backward in time is obtained by replacing F by $-F$.

Zero-Velocity Curves and Libration Points

The surface of zero velocity is obtained by equating the right-hand side of Equation (5) to zero, which gives

$$T = (16/D)\ (ch\,F - \gamma\ \cos E) + (1/2)\ (ch\,2F + \cos 2E) + 2\gamma\ chF\ \cos E.$$

Its E-profile is, setting $F = 0$ and $R = \cos E$,

$$T = (16/D)(1 - \gamma R) + R^2 + 2\gamma R \tag{8a}$$

with minimum at

$$\gamma = R(16 + D^2)/[8(1 + R^2) - D^2] \tag{8b}$$

with $D = 1 - R^2$.

The F-profile is, setting $E = 0$ and $R = chF$,

$$T = (16/D)(R - \gamma) + R^2 + 2\gamma R \tag{9a}$$

with minimum at

$$\gamma = [8(1 + R^2) - RD^2]/(D^2 + 16R) \tag{9b}$$

with $D = R^2 - 1$.

But the condition for a libration point is that $\partial U/\partial \xi = 0$ and $\partial U/\partial \eta = 0$. From Equation (5) we see that this corresponds to a minimum of the zero velocity surface. The above profiles have been calculated for various values of γ and are referred to in the text below as *zero-velocity curves*. For each R, a value of γ has been calculated from (8b) and (9b) and the corresponding minimum value of T from (8a) and (9a). The resulting profiles are the loci of L_1 and L_2 and are referred to as *libration curves*. The data are given in the first two tables and also graphically.

Motion near Libration Points[(4)]

Let us assume $\xi = \xi_0 + X$, $\eta = \eta_0 + Y$ where ξ_0, η_0 denote a libration point and X and Y are small. The equations of motion are then

$$\left.\begin{aligned} \ddot{X} - 2\dot{Y} &= U_{\xi\xi}X + U_{\xi\eta}Y \\ \ddot{Y} + 2\dot{X} &= U_{\xi\eta}X + U_{\eta\eta}Y. \end{aligned}\right\} \tag{10}$$

The second derivatives of U are as follows:

$$\left.\begin{aligned} U_{\xi\xi} &= 1 - \frac{4(1+\gamma)}{r^5}[\eta^2 - 2(\xi + r_1)^2] - \frac{4(1+\gamma)}{\varrho^5}[\eta^2 - 2(\xi - r_2)^2] \\ &= 1 + 2A \quad \text{for} \quad \eta = 0 \\ &= 3/4 \quad \text{at} \quad L_4 \end{aligned}\right\} \tag{11a}$$

where $A = \dfrac{4(1+\gamma)}{r^3} + \dfrac{4(1-\gamma)}{\varrho^3}$,

$$\left.\begin{aligned} U_{\xi\eta} &= 12(1+\gamma)(\xi + r_1)(\eta/r^4) + 12(1-\gamma)(\xi - r_2)(\eta/\varrho^4) \\ &= 0 \quad \text{for} \quad \eta = 0 \\ &= \frac{3\sqrt{3}}{2} \quad \text{at} \quad L_4 \end{aligned}\right\} \tag{11b}$$

and

$$\left.\begin{aligned} U_{\eta\eta} &= 1 - \frac{4(1+\gamma)}{r^5}\left[(\xi + r_1)^2 - 2\eta^2\right] - \frac{4(1-\gamma)}{\varrho^5}\left[(\xi - r_2)^2 - 2\eta^2\right] \\ &= 1 - A \quad \text{for} \quad \eta = 0 \\ &= 9/4 \quad \text{at} \quad L_4 . \end{aligned}\right\} \tag{11c}$$

The quantity A may be evaluated as a function of R by substituting the values of γ from (8b) and (9b). For $R^2 < 1$, i.e., L_1, we find

$$A = 8(7 + R^2)/(7 + 10R^2 - R^4) \tag{12}$$

so that the values decrease from 8 at $R = 0$ to 4 at $R^2 = 1$.
For L_2, $1 \leq R \leq 3$, with $D = R^2 - 1$

$$A = 32\left[R + \frac{2}{R+1}\right]/(D^2 + 16R). \tag{13}$$

The values of A decrease steadily from 4 at $R = 1$ to 1 at $R = 3$, which corresponds to γ going from $+1$ to -1. In other words, $A \geq 1$ at the libration points L_1, L_2 and L_3.

Case I: Libration Point on ξ-Axis

When the libration point is on the ξ-axis, $U_{\xi\eta} = 0$ and Equations (10) become

$$\left.\begin{aligned} \ddot{X} - 2\dot{Y} &= (1 + 2A)X \\ \ddot{Y} + 2\dot{X} &= (1 - A)Y \end{aligned}\right\} \tag{14}$$

Let $X = ae^{mt}$ and $Y = be^{mt}$.
Then $am^2 - 2bm = (1 + 2A)a$

$bm^2 + 2am = (1 - A)b$

$$b/a = \frac{m^2 - (1 + 2A)}{2m} = \frac{-2m}{m^2 - (1 - A)}$$

and $m^4 + (2 - A)m^2 + (1 + 2A)(1 - A) = 0$.
Solving, $2m^2 = A - 2 \pm (9A^2 - 8A)^{1/2}$.
Since $A \geq 1$, $m = +\varrho, -\varrho, i\sigma$, or $-i\sigma$
where $2\sigma^2 = 2 - A + (9A^2 - 8A)^{1/2}$.
If $A = 1$, $\sigma = 1$ and the period is 2π; such motions belong to class (a). If $m = -\varrho$, the motion leaves the libration point in an asymptotic orbit. The slope is determined by the value of γ, and hence one can obtain periodic asymptotic orbits for just special values of γ. These are then of minor significance in comparison with the classes which vary continuously with γ.

Case II: Motion near L_4 (or L_5)

At L_4, Equations (10) become

$$\left.\begin{aligned}\ddot{X}-2\dot{Y}&=\alpha X+\beta Y\\ \ddot{Y}+2\dot{X}&=\beta X+\delta Y\end{aligned}\right\}\qquad(15)$$

where $\alpha=\frac{3}{4}$, $\delta=\frac{9}{4}$, $\beta^2=\frac{27}{16}\gamma^2$.

Then $am^2-2bm=\alpha a+\beta b$, $bm^2+2am=\beta a+\delta b$,

$$\frac{b}{a}=\frac{m^2-\alpha}{2m+\beta}=\frac{-2m+\beta}{m^2-\delta},$$

and $m^4+m^2+\frac{27}{16}(1-\gamma^2)=0$, the roots of which are

$$m^2=-\frac{1}{2}\pm\frac{1}{2}\left[1-\frac{27}{4}(1-\gamma^2)\right]^{1/2}.$$

This will be real for $|\gamma|\geq(23/27)^{1/2}=0.922958$, but complex otherwise. When m^2 is real, it is negative and the trajectory will be an ellipse in the ξ, η plane.

Let us suppose $m=-p+iq$, a complex number, and that

$$X=e^{-pt}(A\cos qt+B\sin qt)$$

$$Y=e^{-pt}(C\cos qt+D\sin qt).$$

Then

$$\dot{X}=e^{-pt}[(-pA+qB)\cos qt+(-pB-qA)\sin qt]$$

and

$$\begin{aligned}\ddot{X}=&\,e^{-pt}\cos qt\,[(p^2-q^2)A-2pq\,B]\\&+e^{-pt}\sin qt\,[(p^2-q^2)B+2pq\,A]\end{aligned}$$

with corresponding expressions for $\dot{Y}$ and $\ddot{Y}$.
If $X=0$ at $t=0$, then $A=0$, and $Y_0=C$, so

$$-2pqB-2(-pC+qD)=\beta C\qquad(16)$$

and

$$(p^2-q^2)B-2(-pD-qC)=\alpha B+\beta D.\qquad(17)$$

Note that $p^2-q^2=-\frac{1}{2}$, $4pq=\left[\frac{27}{4}(1-\gamma^2)-1\right]^{1/2}$.

Also, at $t=0$, the slope is

$$\frac{dY}{dX}=\frac{-pC+qD}{qB}=-p-\frac{\beta}{2q}\frac{C}{B}.\qquad(18)$$

If $\gamma = 0$, then $\beta = 0$, and the initial slope equals $-p$ from Equations (16) and (18). Equations (16) and (17) can be rewritten as

$$-2\,pqB - \theta C = 2\,qD$$

$$-\frac{5}{4}B + 2\,qC = \theta D, \quad \text{with} \quad \theta = -2\,p + \beta.$$

From this,

$$\frac{C}{B} = 2\,q\,\frac{-p\theta + \frac{5}{4}}{\theta^2 + 4\,q^2}.$$

Therefore,

$$\frac{dY}{dX} = -p - \beta\,\frac{-p\theta + \frac{5}{4}}{\theta^2 + 4\,q^2}. \tag{19}$$

(This holds for an incoming orbit.)

For an outgoing orbit, replace $-p$ by p in θ and in Equation (19).

The Jacobi integral at L_4 is obtained by setting $\xi = \gamma$, $\eta = \sqrt{3}$ in $2U$, and is $K = 11 + \gamma^2$. For comparison of asymptotic orbits with various γ, it is convenient to use the quantity $T = K - \gamma^2$, since this is always equal to 11 at L_4.

Limiting Periodic Motions

When $\gamma = -1$, the motion in the fixed system will be an ellipse around the origin. If the eccentricity $e = 0$, then the motion will be circular in the rotating frame also. But if $e \neq 0$, the motion in the rotating system will be closed only if the periods in the fixed and rotating systems are commensurate.

Let $J = r^2\dot{\theta}$ = angular momentum in the fixed system and consider the motion for $\gamma = -1$. From Equation (2), we have $\dot{r}^2 + r^2\dot{\theta}^2 - (16/r) = 2\,h$, where h = total energy. At the ends r_1 and r_2 of the ellipse, $\dot{r} = 0$, and

$$r^2 + \frac{8}{h}r - \frac{J^2}{2\,h} = 0. \tag{20}$$

The sum of the roots will be the major axis,

$$r_1 + r_2 = 2\,a = -8/h, \quad \text{or} \quad a = -4/h \tag{21}$$

and the product

$$r_1 r_2 = a(1-e)\,a(1+e) = -J^2/2\,h = J^2 a/8.$$

Therefore

$$J^2 = 8\,a(1-e^2) = 8\,b^2/a. \tag{22}$$

From Equations (3) and (20) with $\dot{\xi} = 0$, $\dot{\eta} = r(\dot{\theta} - 1) = (J/r) - r$, $\xi = r$, $\eta = 0$, we have

$$-K = \dot{\eta}^2 - (16/r) - \xi^2 = (J^2/r^2) - (16/r) - 2J = 2h - 2J$$

or

$$K = -2h + 2J \tag{23}$$

or

$$K = T + 1 = -2h \pm 2r[2h + (16/r)]^{1/2}. \tag{24}$$

When $e = 0$, $r = a$, $h = -4/r$, and Equation (24) reduces to

$$K = (8/r) \pm 4(2r)^{1/2} = T + 1. \tag{25}$$

The initial velocity $\dot{\eta} = [2h + (16/r)]^{1/2} - r$ when $J > 0$, and will be zero when

$$r^3 - 2hr - 16 = 0. \tag{26}$$

For a value of r satisfying Equation (26), the profile of the class touches the zero-velocity curve (z.v.c.) and the motion changes from retrograde to direct, or vice versa. If $e = 0$, this happens for $r = 2$.

For $e = 0$, $E = 0$, and $\dot{F} = 0$, we have $\dot{\eta} = -shF\dot{E}$. With $\dot{E} > 0$ as usual, $\dot{\eta}$ is opposite in sign to F. Therefore, since $\dot{\eta} = \pm(8/r)^{1/2} - r$, F will be negative when $J > 0$ and $r < 2$, but positive otherwise. This negative profile for $r < 2$ is one branch of the (g) class, starting from $r = 0$, $T = \infty$, and ending at $r = 2$, $T = 11$, and is shown as Curve J in Figure 11. Its extension, $2 \le r < \infty$, corresponds to circular orbits around both masses, direct in the fixed system [(l) class]. If $J < 0$, the orbit is retrograde in the fixed system, belonging to the (f) class when $r < 2$ and to the (m) class when $r > 2$.

When $e \neq 0$, the commensurability condition is to be applied. In the fixed system, the rate at which area is swept out is $J/2$. Since the area of an ellipse is π a b, the period will be, from Equation (22),

$$P = \pi(a^3/2)^{1/2} = \pi(-32/h^3)^{1/2}.$$

If we set this equal to $2\pi/n$, where n is the ratio of two integers, then

$$h^3 = -8n^2. \tag{27}$$

This equation, substituted in Equation (24), gives a relation between K (or T) and ξ (or r). Each value of n describes a class, and the K *vs* ξ relation determines the E- and F-profiles. The third table gives the values of n for some of the classes. If the profile for some class is known, the collision orbit (for $\gamma = -1$) has $K = -2h$, and we can calculate n from Equation (27). If the collision orbit is not known, then $-2h$ can still be found by solving the quadratic equation $(K + 2h)^2 = 8hr^2 + 64r$, if two pairs of values of K and r are known. (Two pairs are necessary in order to choose the proper sign, in the quadratic solution, that keeps h constant.)

As we have defined a class, it is represented uniquely by an eigensurface relating T, E, F, and γ. If it has a section (profile) at $\gamma = -1$ or $\gamma = +1$, then the *rational number* n in Equation (27) is an *invariant* of this section. That *the symmetry properties are somewhat secondary in characterizing a class* is evident by examining the (α) class, for which $n = 3$. This class had been defined for $\gamma = 0$ as having $\dot{E} > 0$ finally as well as initially. But for $\gamma = -1$ we find a smooth transition, from $\dot{E}_f > 0$ to $\dot{E}_f < 0$, at $T_c(\gamma) \simeq 11.93$, so that above this critical $T_c(\gamma)$ the class takes on the symmetry characteristics of the (δ) class. This hybrid (α–δ) class has no apparent relation to our previous (δ) class, which does not exist for $\gamma < -0.48$, although portions of the two classes lie very close together at $\gamma = 0$.

General Dependence on Mass Ratio γ

The eigensurface of a class involves T, E, F and γ. It is convenient to set $E = 0$ [or $F = 0$] and to consider the ordinary surface (T, F, γ) [or (T, E, γ)]. Assuming that one has obtained a (T, F)-profile for some particular γ, the most rapid way of determining how this profile varies with γ is to hold F fixed and to find the (T, γ) profile. In this way we may learn that the section of the eigensurface with $E = 0$ and γ constant consists of more than one curve and that the profile with which we began is only one branch of the complete (T, F)-profile.

As a first example, consider the (n) class ejection orbits ($E_i = 0$, $F_i = 0$). Starting with $\gamma = -1$, the energy T rises steadily until γ becomes positive, as shown in Figure 1 (Curve D), but turns around and downwards near $\gamma = 0.12$, decreasing until about $\gamma = -0.5$ and reversing again to go to positive values of γ. More reversals probably occur, but they have not been traced. Suffice it to say that there are at least 3 ejection orbits for $\gamma = 0$, one of which is at $T = 8.732$, which belongs to the (c) class of Strömgren. This (c) class is thus that special (n) class which is symmetric about the η-axis *only* when $\gamma = 0$. The *upper* ejection orbit corresponds to the (n) branch already known for $\gamma = 0$, and the lower ejection orbit belongs to an (n) branch not previously studied, but included in our tables here. The (c) class begins at $T = 16$ and decreases, crossing the other two (n) branches and oscillating (see Figure 6).

Consider the crossing of the upper branch, and label the parts of the curves according as they lie to the left or right of the crossing point by n_l, c_l, n_r, and c_r. If γ becomes positive, the result is a left-hand curve and a right-hand curve, going in the limit as $\gamma \to 0$ into $n_l + c_l$ and $n_r + c_r$, respectively. On the other hand, if γ becomes negative, the result is an upper curve and a lower curve, with limits $n_l + c_r$ and $c_l + n_r$, respectively. We shall call these two modes of separation the right-left mode and the upper-lower mode. In general, *as γ changes continuously in one direction, two branches, or two parts of one branch, of a class may move toward each other, touch, and separate in the other mode.*

Let us consider in detail how this behavior comes about and what its consequences are. Suppose that, as γ increases, two (T, F) curves more vertically toward each other, touch at (γ_0, T_0, F_0) and then separate in the right-left mode. Let F_1 and F_2 be arbitrary values of F_i, such that $F_2 > F_1 > F_0$. For $F_i = F_0$, the (T, γ) profile turns around at $\gamma = \gamma_0$, but for $F_i = F_1$, it reverses at $\gamma = \gamma_1 > \gamma_0$, and for $F_i = F_2$ at $\gamma = \gamma_2 > \gamma_1$. For the (a) class, Curve C of Figure 5 moves upward to meet the upper branch at $\gamma \simeq 0.78$ and then the right-left splitting occurs. Curve B, Figure 1, shows the (T, γ) profile of the (a) class for $F_i = 0.4$, and Curve A, Figure 1, shows it for $F_i = 1.1$. As expected, the reversal of Curve B comes at a value of γ less than that for the reversal of Curve A. However, Curve C of Figure 1 goes steadily toward $\gamma = 1$ without any reversal. This is because Curve D of Figure 5 (left-hand side) crosses the T-axis just once, and never (for $\gamma < 1$) becomes vertical at $F = 0$.

The F-profile ($E_i = 0.0$) ejection orbits for the complex (g) class are partially graphed as Curves E and F, Figure 1. When γ starts at zero and becomes negative, the previously known upper and middle ejection orbits draw together to disappear as a pair near $\gamma = -0.38$. The lower ejection orbit goes, as $\gamma \to -1$, to the ejection orbit associated with $n = 2$. The two lower ejection orbits have not been traced out systematically above $\gamma = 0$, but they have been located at $\gamma = +9/11$ and at $\gamma = 0.93$ (Curves C and D, Figure 12). They are close together and just above Curve C, Figure 1, which behavior will probably be preserved up to $\gamma = 1$. The upper ejection orbit (Curve F, Figure 1) seems to head toward $T = 11$ as $\gamma \to +1$. The initial portion of the (g) class C from $T = \infty$, $F < 0$ corresponding to Curve J ($\gamma = -1$), becomes smaller because the effective range of m_2 decreases as this mass does. (Similar behavior is shown by the (f) class, to be discussed shortly).

Curve G of Figure 1 shows the existence of a *lower* (δ) branch (Curve S, Figure 8) of the $(\alpha$–$\delta)$ class at $F_i = -0.641489$ for $\gamma > -0.72$. The transition of the *upper* branch, as γ increases, from (α)- to (δ)-symmetry occurs for $\gamma \simeq -0.68$ and $T \simeq 12.53$.

The (β) and (δ) classes probably behave similarly as γ becomes more negative. For $\gamma = 0$, the (β) class has an open profile, ending in spirals about points representing asymptotic orbits III and IV of Strömgren. As γ becomes negative, these two points come closer together until they finally coincide for a value of γ about -0.24. [For γ still more negative, these asymptotic orbits (normal to the ξ-axis) do not exist.] As the points come closer, so do the associated spirals until they finally touch. The (β) class then becomes closed (via the upper-lower splitting mode), but surrounds an open spiral branch between III and IV. This in turn closes, and generates another pair of closed and open curves, so that an *infinite nested set of closed curves* evolves as a result of the above coincidence. As γ becomes still more negative, the outer branch shrinks down (and with it the inner branches), finally to disappear at about $\gamma = -0.8$. The (δ) class is already closed at $\gamma = 0$, but surrounds its open (μ) class offspring between orbits I and II, which are close together. (Presumably (δ) opens up as γ becomes positive.) As γ becomes negative and I and II come together, the (k) class will shrink and develop first an outer branch and then the inner progeny.

Structure of Selected Classes

We shall now discuss in detail the structure of six simple symmetric classes, namely (f), (β), (a), (n), $(\alpha–\delta)$, and (g). The (δ) class does not seem to present much of interest, because it just shrinks to zero at about $\gamma = -0.48$. The (k) class stretches between asymptotic orbits I and II, which coalesce for a value of $\gamma \simeq -0.059$, and will shrink down to zero as the (δ) class does, the F-profile for (k) being contained inside that for the (δ) class.

The E- and F-profiles of the **(f) *class*** are shown in Figures 2 and 3. At $\gamma = -1$ they are given by Equations (4) and (25) with the $(-)$ sign and $\xi = r \leq 2$, and are plotted as Curve A on both figures. The curves drop gently from infinite T to a value of $T = -5$ at $E = -\pi$ or $F = \cosh^{-1} 3$. The first minimum value of T increases to -2.9 at $\gamma = -9/11$ (Curve B), then to 3.8 at $\gamma = 0$* (Curve C) and has disappeared at $\gamma = +9/11$ (Curve D), where only an inflection point remains, at $T = 9.2$.

This inflection point separates the region near mass m_2 from an outer region where the influence of this mass is not felt very much. Inside the inflection point, the profile rises sharply to $T = \infty$ at the mass m_2, but as $m_2 \to 0$ the distance out to the inflection point becomes vanishingly small. As $\gamma \to 1$, the profile for the outer region approaches the limiting Curve G, derived from the invariant index $n = 1$ used in Equations (27), (24), and (4). The same F-profile curve also appears to be the limiting profile for the (a) class (see Figure 5), and indeed the libration point L_2 approaches the mass m_2 as that mass becomes vanishingly small. Hence it is not surprising that periodic orbits for (f) and (a) classes approach a common limit when the influence of the mass becomes negligible.

Figure 4 shows how the **(β) *class*** disappears as γ becomes negative and what happens to the nearby portion of the (g) class at the same time. Curve β_0, representing the (β) class at $\gamma = 0$, is open at the bottom and stretches between asymptotic orbits III ($E = 0.8706$) and IV ($E = 0.2957$). Curve g_0 [(g) class at $\gamma = 0$] detours around β_0 and does not intersect it. At $\gamma \simeq -0.24$ and $E \simeq 0.75$, orbits III and IV coalesce, the (β) profile closes off (generating its nested set of inner closed profiles), and then moves downward and to the right. The (g) profile also moves downward, with elimination of the hairpin turns and upward bulge. The curves labelled g and β in the figure show the situation at $\gamma = -0.59$, and the heavy cross shows where, at $\gamma \simeq -0.83$, the (β) class vanishes.

In general, once a class has become closed by a change of γ in some direction, further change of γ in the same direction will bring about its shrinkage to zero. The particular value of γ at which the class disappears does not seem to have any special significance. For instance, the (δ) class vanishes at about $\gamma = -0.48$ and the lower $(\alpha–\delta)$ class at about $\gamma = -0.71$ (see Figure 9).

The development of the ***a* (*class*)** from $\gamma = -1$ to $\gamma = +1$ is illustrated in Figure 5. This class has termination points at L_2, the locus of which has been plotted as

* Data not included in our tables for the $\gamma = 0$ curves (of all the classes discussed here) can be found in Reference 1.

dashed lines; for $\gamma \to -1$, the locus goes to the point $T = 11$, $F = \pm \cosh^{-1} 3$, while for $\gamma \to 1$ the locus goes to $T = 11$, $F = 0$. The limiting profiles at $\gamma = \pm 1$ have both been calculated using the invariant index $n = 1$, and are identified on the figure as Curves H and A, respectively.

The minimum value ($T = -5$) of curve A for $\gamma = -1$ increases to $T \simeq 4.2$ for $\gamma = 0$ (curve B) and to $T \simeq 9.5$ for $\gamma = 9/11$ (upper minimum of curve D). Curve C shows parts of the lower (a) class for $\gamma \simeq 0.63$, now expanding upward shortly after its "birth" at $\gamma \simeq 0.58$. When $\gamma \simeq 0.78$ this lower section, with its two sharp maxima protruding up on the left and right, touches the flattened out upper section, splits away in the left-right mode, and so generates two new sections out of the old pieces. These two sections, a large outer "bag" (incomplete) and a smaller inner "island" (closed), are shown for $\gamma \simeq 0.82$ as Curve D in the figure. At this value of γ, we see two channels between "island" and "bag", and the right one is especially narrow. A tiny loop occurs at the bottom of the "island", indicating that cusps and loops can occur in the (T, F) [or (T, E)] plane, completely analogous to orbital loops in the (E, F) plane.

As γ increases, the inner "island" probably shrinks to nothing. The upper portions of the outer "bag", hanging suspended from the L_2 locus, gradually slide down the locus to the singular point at $T = 11$. Curve G shows part of the outer "bag" for $\gamma = 0.93$, a close bounding surface now for the (g) class. As $\gamma \to 1$ the outer portion of the "bag" tends toward Curve H, while the inner vertical portion goes toward the T-axis.

Figure 6 shows how the ***(n) class*** begins to develop. (Since E runs from 0 to -2π, we need only study the range $0 \leq \gamma \leq 1$.) The 3 branches at $\gamma = 0$ are indicated by dashed lines, u denoting the upper, c the middle, and l the lower branch, respectively.

The upper and lower branches are non-intersecting sinusoidal-like curves with period 2π. They are intersected four times (P, Q, R, S) by the middle (c) branch, which begins at L_1 and drops rapidly in T, oscillating across the other branches in so doing. When γ increases from zero, the intersecting branches break apart. The splitting is left-right at the points marked P and S; the upper-lower splitting mode occurs at points Q and R. The solid lines indicate the 3 rearranged branches at $\gamma = 0.12$, U denoting the upper, M the middle and L the lower branch, respectively. When γ decreases from 0.12 to 0, $U \to cuc$, $M \to uclc$, and $L \to lc$, the limits being curves made up of pieces of the various branches at $\gamma = 0$.

As γ becomes more positive, the M branch shrinks down to curve m at $\gamma \simeq 0.66$ and disappears for $\gamma \simeq 0.7$. The evolution of the U branch is shown in Figure 7. Curve D is the composite of pertinent $\gamma = 0$ pieces from which Curve C (for $\gamma = 0.12$) derives. As γ increases, the minimum value of T decreases to negative values, the two pairs of relative maxima and minima which existed at $\gamma = 0.12$ disappear, and the U branch goes smoothly into Curve B as $\gamma \to 0.90$. This branch begins and ends on the locus for L_1 (shown in dashed lines), just as the (a) class is attached to the L_2 locus. As $\gamma \to 1$ the end points slide down the L_1 locus to the points at $T = 11$. The middle portion of the profile goes smoothly into limiting Curve A, which is calculated using the invariant index $n = 5/3$ in Equations (24) and (27).

A general set of profiles for the **(α–δ) *class*** is given in Fig. 8. Curve A, the limiting profile at $\gamma = -1$, has the invariant index $n = 3$ and is tangent to the zero velocity curves at $T_c \simeq 11.93$. For $T > T_c$ the trajectories have (δ)-type symmetry ($\dot{E}_f < 0$), while for $T < T_c$ they have (α)-type symmetry ($\dot{E}_f > 0$). There is a *continuous transition* at $T = T_c$ from one type to the other, which comes about as follows. The (α)-trajectory (during the final part of the half-period) crosses the F-axis with $\dot{E} < 0$ at some value $F_k < F_f$, then turns and comes back to the F-axis at $F = F_f$, with $\dot{F}_f = 0$, $\dot{E}_f > 0$, forming half of a loop. As T approaches T_c from below, F_k approaches F_f, the loop constricts and at $T = T_c$ we have $\dot{E}_f = 0$, $\dot{F}_f = 0$, i.e., when the loop has shrunk to zero, the orbit has a cusp at the zero-velocity curve. If T now increases above T_c, the cusp irons out, $\dot{E}_f < 0$, and the class is of (δ)-type.

As γ increases from -1, the (α–δ) class develops in a rather complicated way, as shown in Figures 8, 9, and 10 by the sequence of profiles A, S, B, P, R, M and N, L and H and Q, K, C and V, and D, corresponding to γ-values of -1, -0.7096, -0.6893, -0.5459, -0.5419, -0.5146 and -0.5183, -0.4839, -0.4025, 0, and 0.8609, respectively. One reason for the complication is the birth*, slightly below $\gamma = -0.71$, of a nested set of profiles associated with asymptotic orbits XI and XIV. The outermost profile of this set is shown as curve S ($\gamma = -0.7096$) and is of δ_2-type. (The subscript denotes the number of intersections, including the beginning, of the half-orbit with the F-axis). Inside this profile there follow in order α_3, δ_4, etc. This set swells up as γ increases, and R shows the δ_2-profile at $\gamma = -0.5419$. On further expansion, when $\gamma \simeq -0.54$, this profile touches the upper branch (approximately at P) at 2 conjugate points, where splitting in the left-right mode then occurs. One new branch is the island M ($\gamma = -0.5146$) which quickly shrinks down and disappears as γ increases. The branch M ($\gamma = -0.5183$) at the right is in the shape of a hairpin above $T = 12$. The right prong belongs to the α_3-class up to $T_c \simeq 12.88$, where the transition to the δ_2-class occurs. From this point on, each point of the hairpin has a conjugate point on the left-hand side of the figure. Conjugate to the transition point is a point on the zero-velocity curve (z.v.c.) from which the δ_2-profile issues tangentially, to the right and upward. After the maximum value of T, this profile turns around and again goes toward the zero-velocity curve, narrowly misses it and turns to follow Curve R to a minimum where the conjugate points meet.

As R swells up, the curves inside it do, too. The next one, α_3, is shown as N, for $\gamma = -0.5183$, in Figures 9 and 10. The right side of Figure 10 shows the hairpin M on an expanded scale, with the Curve N running parallel to it for a while, and very close.

The z.v.c. (Curve m) has a minimum at $T \sim 12.6767$, and Curve N lies just below with $T \simeq 12.6754$, the separation being too small to appear on the graph. (Curve N, Figure 10, left side, is just a mirror image of the usual α-profile; the actual eigensurface here is continuous with $F > 0$).

* Asymptotic orbits XIV and XI first appear at $\gamma \sim -0.582$, $F \simeq -0.35$ ($T = 11$) and are represented at $\gamma = 0$ by $T = 11$, $F = -0.8124$ and 0.4065, respectively.

As γ increases above -0.5183, Curve N rises to meet the z.v.c., and the resulting point of tangency marks the boundary between α_3- and δ_2-symmetry. Curve M (δ_2-part) has moved over to touch N at this same place, and thus four branches all meet here (See Figure 10, left side). Recombination can now occur, upper N with lower M and upper M with lower N, giving 2 (α–δ) curves, each with its own point of tangency to the z.v.c. [note that lower N on the left side corresponds to upper N on the right side, and vice versa]. The upper curve evolves to Curve LH at $\gamma = -0.4839$, and the lower curve to Q, which must now have just one type of symmetry (in fact δ_2) since it does not touch the z.v.c. any longer. Curve Q has only been traced out partially, and the details of its breakaway from the z.v.c. have not been studied.

The important feature of Curve LH is that it is tangent to the z.v.c. at two points, so that there is a transition from α_3-type to δ_2-type at one point and the reverse transition at the other point. As γ increases, the portion with δ_2-symmetry becomes smaller and finally vanishes, after which the profile pulls away from the z.v.c.

By the time γ has increased to -0.4839, α_3 has developed a pronounced minimum which is shown on Figure 9 by Curve H. This may be visualized as a depression that is being produced by the rapid expansion of the original (δ) class, which is shown for $\gamma = -0.40245$ as Curve G. This expansion continues with increasing γ, making it difficult to locate the minimum T for the α_3 class. Consequently, only right and left branches are shown for $\gamma = -0.40245$ (Curve K) and $\gamma = 0$ (Curve C). The left branch of Curve C is bounded on the left by the δ_2-profile for $\gamma = 0$, Curve V, which has evolved continuously from Curve S ($\gamma = -0.7096$). Curves S and B are fairly far apart, but Curve V approaches the right branch of Curve C rather closely.

Part of the profile at $\gamma = 0.8609$ has been run out, and is shown as Curve D on Figure 8. The minimum of T has increased greatly, and the valley is not so wide, which is probably due to increasing constriction by its z.v.c. (Curve d). The z.v.c. at $\gamma = 1$ is shown as dashed Curve e.

Turning now to the ***(g) class***, let us see how the profiles change. At $\gamma = 0$, the profiles come from $T = \infty$, intersect the (δ) class at top and bottom, go around the (β) class and, after going through a minimum and a maximum, terminate in a spiral around an asymptotic orbit. As γ becomes negative the (δ) class shrinks, and disappears at about $\gamma = -0.484$. At the same time the corresponding (F-profile) pocket of the (g) class also vanishes. (See Figure 11). The E-profile still must curve to avoid the (β) class. However, the (β) class becomes closed and also shrinks down as γ becomes more negative. The E-profile, for $E > 0$, smooths out, as shown by Curve g, Figure 4 ($\gamma = -0.59$) and by Curve A, Figure 13 ($\gamma = -9/11$).

For $F > 0$ (or $E < 0$) Curve A goes through a minimum and rises very steeply. The eigensurface meets the zero-velocity surface tangentially, as shown on the F-profile, Curve A, Figure 11. The symmetry then changes to that of the (f) class, but the termination of the E-profile is no longer on asymptotic orbit VIII as it was at $\gamma = 0$.

To ascertain how the manner of termination changes, special computations were carried out. Starting after the maximum of the E-profile with $E_i = -1.88785$ and keeping T constant at 11, E was found as a function of γ down to $\gamma \simeq -0.9468$. Then, starting at $T = 11$ and holding γ constant at -0.9468, the E-profile was run up past the maximum and to the right, to give a *closed* branch of the (g) class (shown as Curve H on Figures 11 and 13) completely *separate* from the branch described above for $\gamma = -9/11$.

This closed branch may be regarded as analogous to Curve S of the $(\alpha-\delta)$ class (Figure 8). As γ becomes more positive, Curve H expands to meet the zero-velocity curve and the main branch. Although the process has not been traced in detail, there is a splitting and recombination so that the left-hand side of the closed branch combines with the right-hand (g) branch represented by Curve A, Figure 13. Along with this, asymptotic orbit VIII and its conjugate VIII* are born at $\gamma \simeq -0.7$, $E \simeq -2.27$, and move apart. (At $\gamma = 0$, $T = 11$, $E = -1.881$ for VIII and $E = -1.791$ for VIII*). This causes the closed branch to open up, and Curve A to end in a spiral about orbit VIII for somewhat higher values of γ. We have not attempted to trace that branch of class (g) which spirals out from VIII*, partly because very tight hairpins seem to be involved (as in the behaviour of the nested profiles of the $(\alpha-\delta)$ class).

The lower (g) class at $\gamma = -1$ is represented by $n = 2$ in Equation (27), and is shown in Figure 15. Inspection shows several features which are still evident in the (g) class at $\gamma = 0$. Starting with Curve 1 at $F \simeq -1.658$, which has cusps on both E- and F-axes (zero-velocity points), the class develops as shown by Curves 2–13. A loop appears and becomes larger with increasing F until there is a double collision orbit at $E = 0$, $F = 0$, and $T = 5.3496$. The angular momentum J (fixed system) now becomes negative and the loop becomes still larger, encircling the origin. The final E intercept decreases steadily to $E = -\pi$, corresponding to $F \simeq 1.76275$ ($\xi = -2$), after which the partial orbit is represented as terminating on the line $E = -\pi$ with $F < 0$ and $\dot{F} = 0$. The initial value of F increases to a maximum at $F \simeq 1.931$, where $J = 0$, $T = 5.3496$, and there is a skew collision orbit (cf. Figure 8c for $\gamma = 0$)[1]. After the maximum, F_i decreases to about 1.658, at which point the velocity is zero again.

There is no (f) class corresponding to $n = 2$, as is shown by the following argument. The motion is uniquely determined by the initial coordinate r and the value of J, because the initial velocity $\dot{\eta} = (J/r) - r$. In the above description of the (g) class, the value of $\dot{\eta}$ started with zero, went positive to a maximum, then through zero to a negative minimum and then back to zero. All values of r and J for $n = 2$ were covered, and all orbits were found to belong to the (g) class, so no others can exist. If, for example, $\dot{F} = 0$, $E = 0$, and $\dot{\eta} = -\dot{E}$ sh F initially and $\dot{E} = 0$, $F = 0$, and $\dot{\eta} = -\dot{F} \sin E$ finally, and we notice that $\dot{\eta}$ changes sign after $P = \pi/2$, then $\dot{E}_i > 0$ and $F_i < 0$ imply that $\dot{F}_f > 0$ for $E_f > 0$, which is g-symmetry.

However, we did find that the (g) class at $\gamma = -9/11$ assumes f-type symmetry after going through a cusp on the F-axis (zero velocity). There is no contradiction, because at $\gamma = -1$ the critical orbit for $n = 2$ has cusps on both E- and F-axes *simultaneously* and thus the symmetry does not change. The value $\gamma = -1$ must then be regarded as exceptional.

At $\gamma = -9/11$, after the (g) class has made the transition to the (f) class, a new F-profile lying below that for the (g) class is obtained (see Figure 11, dashed Curve A). Let us denote this by F_1. An (f) class quarter-orbit differs essentially from one for the (g) class only in having a small, final half-loop. The profile F_1 goes from the left-hand z.v.c. more or less parallel to the (g) class profile (F_0) down to a minimum and up again. Because the orbits develop in the same way as those of the (g) class, F_1 will meet the right- hand z.v.c. and turn into a new profile F_2 (g-type). The class never ends, but F_n will probably approach a limiting curve, as $n \to \infty$.

At $\gamma = -1$, the (g) class has 2 branches, Curve K with $e \neq 0$, $n = 2$, and Curve J with $e = 0$. When γ increases from $\gamma = -1$, Curves J and K break apart (in the left-right mode). On the F-profile (Figure 11) the right-hand branch rounds off, moves slowly to the right and becomes Curve A at $\gamma = -9/11$. The left-hand branch shrinks down to disappear at $\gamma \simeq -0.98$.

As γ continues to increase, Curve A is transformed into Curve B at $\gamma = 0$ and into Curve C at $\gamma = +9/11$. After asymptotic orbit VII appears, the upper-right section of the F-profile terminates in a spiral around VII, much as the E-profile does about VIII, and the evolution may be conjectured to be similar. The (g) class profile stays below that of the (α) class profile, which pulls away from the z.v.c. The (g) class is in general intermediate between the (α) class and the (a) class. The latter profile goes between the points representing L_2 and is outside and below the (g) class profile. As γ increases, the (a) class profile pushes upward and the (g) class F-profile goes with it, which accounts for the lower left part of Curve C ($\gamma = +9/11$). The pocket is due to the presence of the (δ) class, and has only shrunk a little at $\gamma = 9/11$. It is still present at $\gamma = 0.93$ (Curve D, Figure 12) and at $\gamma = 0.97569$ (Broucke[(5)]), where the (δ) class must be closed, since asymptotic orbits I and II cannot exist for $\gamma > 0.923$.

The behavior as γ increases beyond $+9/11$ is influenced very greatly by the appearance of at least one, but probably two lower branches of the (g) class, and the interaction with the upper branches is best seen by referring to the E-profile (Figure 14). One lower branch, Curve G for $\gamma = +9/11$, has a sharp peak at maximum T. As γ increases, this thrusts up to meet the upper branch (Curve C) near $E = -1$, and a left-right splitting ensues. A similar process evidently occurs near $E = +0.3$, so that Curve D for $\gamma = +0.93$ has two long appendages which go down to low values of T. They are thin on the E-profile, but broad on the F-profile (Figure 12). At $\gamma = +9/11$, the F-profile for that lower branch corresponding to $E \simeq 0.3$ must lie inside Curve G, so that its meeting and splitting with the pocket of Curve C will occur after the left-right splitting of G and the lower portion of Curve C.

Attempts were made to find the limit of the (g) class profiles as $\gamma \to 1$, but these did not yield any definite result. High accuracy of integration is required, and other as yet unknown branches probably appear. In the event that the determination of this limit should prove important, it is likely that the investigation will require at least as much effort as was spent on the (α–δ) class.

Broucke[5] has calculated 392 periodic orbits for $\gamma = \pm 0.97569$ (Earth-Moon system). The correspondences are:

Class	(f)	(g)	(a)	(n)
$\gamma = 0.97569$	C	H_1, H_2	J_1	G
$\gamma = -0.97569$	A_1	BD	I	

where the capital letters denote "families" of Broucke. The family H_1 is the beginning of class (g), and resembles that part of Curve D, Figure 12, with collision orbit at $T \simeq 12.27$. The class goes to very low values of T and so was apparently "lost" by Broucke, who picked it up on the return (left upward prong of Curve D) and labelled it as the family H_2. This, too, was lost on the downward plunge, and the right-hand branch of Curve D was not discovered. It is precisely here that additional work is necessary to ascertain what happens as $\gamma \to 1$.

Conclusions

The present work has been concerned with the evolution of several simple symmetric classes. The results may be summarized as follows:

1. When the mass-ratio changes, two branches of an eigensurface may move toward each other, touch, and split into two other branches which then move apart.
2. This interaction may occur when both branches touch the zero-velocity surface, in which case the relations are somewhat complicated.
3. When the eigensurface touches the zero-velocity surface, a change of symmetry (reversal of velocity) occurs, as from g to f and from α to δ.
4. Asymptotic periodic orbits appear and disappear in pairs. The (g) class at $\gamma = 0$ appears to terminate on asymptotic orbits VII and VIII, but there are in fact additional branches associated with orbits VII* and VIII*.
5. The (g) class at $\gamma = -1$ consists of at least 2 branches, one with $e \neq 0$ and invariant index $n = 2$, and the other with $e = 0$ ($r < 2$). As the mass-ratio varies from $\gamma = -9/11$ to $\gamma = -1$, the F-profile changes continuously from Curve A (Figure 11) to Curve JK, composed of parts of these 2 branches. Since Curve JK does not appear to possess any single quantity which is invariant over the whole of the curve, it is unlikely that Curve A (typical for $\gamma \neq -1$) has an invariant, either.
6. The main features of classes (a), (f), and (n) have been found for the whole range $-1 \leq \gamma \leq 1$, and those of classes (β), (δ), (α–δ), and (g–f) for $-1 \leq \gamma \leq 0.93$. The vicinity of $\gamma = 1$, if of interest for these latter classes, would require a separate investigation.

Acknowledgements

This work was begun at the Copenhagen Observatory, the facilities of which were kindly extended to us by Professor ANDERS REIZ. Valuable results for the (n) class and for the $(\alpha\text{–}\delta)$ class were obtained with the aid of the GIER computer, made available to the Observatory by the Carlsberg Foundation.

After the new program had been written for the IBM 7094 at Illinois, Mr. ANIL RAHEJA rendered valuable assistance in tracing out the classes. The figures were prepared by Mr. YUI-KEUNG LI, whom we are pleased to thank for his excellent draftsmanship.

The senior author (J.H.B.) had the benefit of a leave from the University of Illinois, and the junior author a fellowship from the National Science Foundation. The research was supported in part by the National Aeronautics and Space Administration (Grant NsG 280–62).

We are truly grateful to these people and agencies for their assistance.

Appendix–Method of Integration

After exploratory work was done on the GIER computer at Copenhagen, obtaining one periodic solution at a time, a new program was written for the IBM 7094 at Illinois. This was designed to run out a profile automatically, and managed this successfully except at sharp hairpin curves, where special analysis was usually necessary.

The equations of motion, Equations (6) and (7), were integrated numerically using a modified RUNGE-KUTTA-GILL program. The first integral, Equation (5), was used to calculate one of the initial velocities from chosen values of the other variables and parameters, and also served as a check on the value of T for each calculated point of the orbit. The deviation from constancy was thus a measure of the overall accuracy of the integration.

As an example, consider the procedure for the (a) class (F-profile). Integration was carried out (with steps $\Delta\psi = 0.02$, fixed) from initial $E = 0$, $\dot{F} = 0$ until $E = 0$ was reached again (interpolating during the last step) and the initial value of F adjusted until the final value of $\dot{F}$ was close to zero. On the IBM 7094 the maximum allowable deviation was usually $|\dot{F}| = 5 \times 10^{-4}$, although in sensitive regions this was increased to as much as 5×10^{-3}.

Once one solution had been found, another of the variables, say T, was incremented and then held constant while the other variable, say F_i, was varied to generate a second periodic solution. After three or more solutions had been found, the profile was extrapolated. Suitable increments were determined from the curvature of the profile, decreasing as the curvature increased.

Appendix–Limiting Motions

For elliptical motion in the fixed system, $x = a\ (\cos \varepsilon \pm e)$, $y = b \sin \varepsilon$, and $nt = \varepsilon \pm e \sin \varepsilon$, where ε is the eccentric anomaly. The coordinates in the rotating system are $\xi = x \cos t + y \sin t = ch\, F \cos E + \gamma$ and $\eta = -x \sin t + y \cos t = -\text{sh}\, F \sin E$. Then, for $\gamma = -1$, $(\xi+1)^2 + \eta^2 - 1 = \text{sh}^2\, F - \sin^2 E$ and $\eta^2 = \text{sh}^2\, F \sin^2 E$. When ξ and η are known, we can solve these equations for $\text{sh}^2 F$ and $\sin^2 E$ and so obtain E and F, except for minor ambiguities which can be resolved by knowing the class and by requiring continuity of motion. Starting with a permissible initial value of ξ and with $\eta = 0$, $\dot{\xi} = 0$, and $n = 2$, one can calculate the subsequent values of E and F as functions of ε. Figure 15 shows the resulting trajectories for selected values of F_i and J, and these curves [for the (g) class] have been discussed in the text.

Department of Physics,
University of Illinois,
Urbana, Illinois, U.S.A.

References

1. J. H. Bartlett: "The Restricted Problem of Three Bodies", Mat. Fys. Skr. Dan. Vid. Selsk., 2, No. 7 (1964).
2. G. Shearing: "Computation of Periodic Orbits in the Restricted Three-Body Problem, Using the Mercury Computer", (Ph. D. Thesis) University of Manchester (1960).
3. T. N. Thiele: "Recherches numeriques concernant des solutions périodiques d'un cas spécial du problème des trois corps" (Troisième Mémoire), Astronomische Nachrichten, 138, Nr. 3289 (1895).
4. See, for instance, F. R. Moulton: "Periodic Orbits", Carnegie Institution of Washington (1920).
5. R. Broucke: "Recherches, d'orbites periodiques dans le problème restreinte plan (système terre-lune)", Dissertation, Université Catholique de Louvain (1962).

(γ, T, E) Locus for Libration Point L_1

Note: To obtain the remainder of the locus, subtract the given E values from π and change the sign of γ.

(Figure 7)

γ	T	E
1.0000	11.0000	0.0000
0.9999	11.0036	0.2000
0.9999	11.0178	0.3000
0.9996	11.0541	0.4000
0.9985	11.1339	0.5000
0.9956	11.2715	0.6000
0.9889	11.4899	0.7000
0.9753	11.8088	0.8000
0.9501	12.2437	0.9000
0.9066	12.7993	1.0000
0.9009	12.8612	1.0100
0.8775	13.1010	1.0470
0.8207	13.5920	1.1180
0.7995	13.7515	1.1400
0.7318	14.1956	1.2000
0.5850	14.9208	1.3000
0.3951	15.5325	1.4000
0.3087	15.7192	1.4400
0.2174	15.8622	1.4800
0.1228	15.9564	1.5200
0.0000	16.0000	1.5708

(γ, T, F) Locus for Libration Point L_2

(Figure 5)

γ	T	F
1.0000	11.0000	0.0
0.99999	11.0249	0.2000
0.9996	11.0534	0.4000
0.9988	11.1162	0.4900
0.9944	11.3033	0.6224
0.9832	11.5925	0.7500
0.9600	11.981	0.8670
0.9334	12.2999	0.9444
0.9303	12.3327	0.9516
0.9064	12.5545	1.0000
0.8770	12.7818	1.0470
0.8140	13.1582	1.1230
0.7265	13.5225	1.2000
0.5689	13.9039	1.3000
0.3515	14.0777	1.4000
0.2179	14.0466	1.4500
0.0000	13.8272	1.5206
−0.1012	13.6658	1.5500
−0.2089	13.3653	1.5800
−0.2906	13.2768	1.6015
−0.3234	13.1989	1.6100
−0.3563	13.1177	1.6180
−0.3894	13.0332	1.6260
−0.4894	12.7602	1.6500
−0.6582	12.2435	1.6890
−0.8287	11.6548	1.7270
−1.0000	11.0000	1.7630

Two-Body $(\gamma = 1)$ Limits for the Classes

Class Name	Invariant Index n	Total Energy h	Energies at Ejection $(F = 0)$ T $(r = 2)$	
a	1	−2.00000	11.0000	−5.0000
n	5/3	−2.81194	10.7898	−1.5420
α–δ	3	−4.16017		
λ	1/2	−1.25992	10.8837	7.8441
$g(K)$	2	−3.17480	10.4883	0.2109

Classes with Zero Eccentricity $(e = 0)$

$g(J)$	$J > 0$	$r \leq 2$
l	$J > 0$	$r \geq 2$
f	$J < 0$	$r \leq 2$
m	$J < 0$	$r \geq 2$

Class (f)

Initial Conditions: $F_i = 0;\ E_i < 0;\ \dot{E}_i = 0;\ \dot{F}_i > 0.$

Final Conditions: $E_f = 0;\ F_f > 0;\ \dot{F}_f = 0;\ \dot{E}_f > 0.$

Note: This class is also represented by the conditions

$$E_i' = 0;\ F_i' > 0;\ \dot{F}_i' = 0;\ \dot{E}_i' > 0.$$
$$F_f' = 0;\ E_f' > 0;\ \dot{E}_f' = 0;\ \dot{F}_f' < 0.$$

To obtain this representation take

$$F_i' = F_f;\ E_f' = -E_i.$$

$\gamma = -9/11$; Figures 2 and 3, Curve B.

** These values have been calculated from the results of Shearing (2).

T	E_i	F_f	$x \equiv \psi$
−2.6450	−2.507181	1.899900	0.5646
−2.6550	−2.494739	1.891087	0.5622
−2.662	−2.469	1.873	**
−2.6450	−2.426279	1.839177	0.5501
−2.609	−2.394	1.818	**
−2.5450	−2.353376	1.792265	0.5388
−2.4450	−2.307158	1.761636	0.5322
−2.157	−2.210	1.704	**
−1.738	−2.101	1.642	**
−1.183	−1.986	1.580	**
−0.492	−1.868	1.513	**
0.331	−1.749	1.446	**
1.281	−1.635	1.373	**
2.350	−1.527	1.306	**
3.529	−1.426	1.240	**
4.809	−1.335	1.177	**
6.182	−1.251	1.118	**
7.640	−1.176	1.063	**
9.179	−1.107	1.012	**
10.795	−1.047	0.964	**
12.486	−0.992	0.921	**
14.250	−0.943	0.880	**

$\gamma = +9/11$; Figures 2 and 3, Curve D.

T	E_i	F_f	x
16.313	−0.460	0.452	**
15.242	−0.499	0.491	**
14.241	−0.547	0.534	**
13.304	−0.602	0.588	**
12.427	−0.673	0.653	**
11.602	−0.766	0.738	**
10.817	−0.892	0.854	**
10.084	−1.075	1.015	**
9.548	−1.285	1.190	**
9.242	−1.450	1.316	**
9.039	−1.575	1.400	**
8.738	−1.761	1.513	**
8.487	−1.900	1.584	**
8.254	−2.009	1.634	**
8.036	−2.100	1.670	**
7.7310	−2.209303	1.710388	0.6661
7.3369	−2.333973	1.749479	0.6369
6.5609	−2.541802	1.802673	0.5979
5.7609	−2.726114	1.838412	0.5726
4.5609	−2.972808	1.868632	0.5507
2.9609	−3.276489	1.878442	0.5394
1.7609	−3.499625	1.869424	0.5401
0.1609	−3.807446	1.837262	0.5518
−0.6391	−3.971542	1.809918	0.5620
−1.2391	−4.102668	1.785905	0.5722
−2.0191	−4.285888	1.748753	0.5881
−2.8038	−4.491600	1.706075	0.6080
−3.6038	−4.732010	1.664361	0.6314
−4.0038	−4.866402	1.650077	0.6432
−4.4038	−5.014286	1.646397	0.6548
−4.8038	−5.175760	1.662969	0.6641
−5.2038	−5.365862	1.716096	0.6711
−5.4038	−5.492277	1.776599	0.6732
−5.4238	−5.509202	1.786455	0.6734
−5.4894	−5.593827	1.844118	0.6737
−5.4633	−5.677202	1.914936	0.6738

Class (β)

Initial Conditions: $F_i = 0;\ \dot{E}_i = 0;\ \dot{F}_i > 0.$

Final Conditions: $E_f = 0;\ \dot{F}_f = 0;\ \dot{E}_f > 0.$

Note: This class is also represented by the conditions

$$E_i' = 0;\ \dot{F}_i' = 0;\ \dot{E}_i' > 0.$$
$$F_f' = 0;\ \dot{E}_f' = 0;\ \dot{F}_f' < 0.$$

To obtain this representation take

$$F_i' = F_f;\ E_f' = -E_i.$$

$\gamma = -0.59$; Figure 4, Curve β.

T	E_i	F_f	x
9.2963	0.460000	1.982249	1.7845
9.3461	0.500000	1.975841	1.8261
9.5351	0.600000	1.961724	1.8945
9.8960	0.800000	1.939736	1.9844
10.0322	0.900000	1.932307	2.0113
10.2000	1.060922	1.924813	2.0153
10.4000	1.204046	1.917884	1.9581

T	E_i	F_f	x
10.6000	1.274974	1.909560	1.8974
11.0000	1.345450	1.888498	1.7879
11.4000	1.369903	1.861224	1.6810
11.8000	1.345141	1.825371	1.5625
11.9000	1.321918	1.814663	1.5279
11.9575	1.300000	1.808252	1.5057
12.0411	1.200000	1.801110	1.4557
11.8388	1.000000	1.835762	1.4347
11.6176	0.900000	1.862266	1.4387
11.3242	0.800000	1.890090	1.4516
11.1868	0.760000	1.901266	1.4596
10.5172	0.600000	1.944597	1.5136
9.9795	0.500000	1.969796	1.5771
9.3461	0.429743	1.986886	1.7171

Class (δ)

Initial Conditions: $E_i = 0$; $\dot{F}_i = 0$; $\dot{E}_i > 0$.

Final Conditions: $E_f = 0$; $\dot{F}_f = 0$; $\dot{E}_f < 0$.

Note: To obtain the remainder of the class take the mirror images, i. e. the values

$$F_i' = -F_f;\ F_f' = -F_i.$$

$\gamma = -0.40245$; Figure 9, Curve G.

T	F_i	F_f	x
13.9764	−0.526881	0.535131	2.5411
13.9519	−0.472471	0.559874	2.5649
13.9279	−0.449193	0.583473	2.5674
13.8849	−0.421283	0.607510	2.5749
13.8525	−0.404716	0.622339	2.5797
13.8130	−0.387436	0.637043	2.5859
13.7657	−0.369430	0.652104	2.5931
13.7114	−0.351314	0.666095	2.6018
13.6507	−0.333276	0.678862	2.6119
13.5849	−0.315709	0.689799	2.6232
13.5143	−0.298567	0.699028	2.6357
13.4400	−0.282021	0.705851	2.6495
13.3624	−0.266090	0.710516	2.6643
13.2838	−0.251043	0.713092	2.6797
13.1982	−0.235745	0.713506	2.6967
13.1482	−0.227288	0.711578	2.7074
13.0982	−0.219051	0.711589	2.7169
13.0382	−0.209600	0.707990	2.7298
12.7600	−0.169920	0.684400	2.7885
12.5257	−0.140828	0.655276	2.8377
12.2413	−0.109812	0.611358	2.8971
12.0032	−0.087090	0.569414	2.9461
11.7654	−0.067284	0.523900	2.9946
11.4705	−0.047140	0.462337	3.0548
11.2930	−0.037872	0.421765	3.0917
11.1182	−0.031521	0.378791	3.1287
10.9487	−0.029107	0.331933	3.1660
10.7895	−0.032225	0.282156	3.2025
10.6478	−0.043715	0.227585	3.2370
10.5376	−0.069520	0.166590	3.2657

Class (α)

Initial Conditions: $E_i = 0$; $\dot{F}_i = 0$; $\dot{E}_i > 0$.

Final Conditions: $E_f = 0$; $\dot{F}_f = 0$; $\dot{E}_f < 0$.

Note: To obtain the remainder of the class take the mirror images, i. e. the values

$$F_i' = -F_f;\ F_f' = -F_i.$$

$\gamma = 0.630199$; Figure 5, Curve C.

T	F_i	F_f	x
−0.2543	1.198858	−2.237951	1.3840
−0.1474	1.205398	−2.232958	1.3789
−0.0625	1.213483	−2.234423	1.3731
0.1332	1.229633	−2.232417	1.3607
0.3260	1.228135	−2.233527	1.3581
0.4856	1.226590	−2.236215	1.3559
0.8537	1.217522	−2.242689	1.3535
1.2408	1.198534	−2.247692	1.3559
1.7752	1.166431	−2.257065	1.3615
2.4262	1.108485	−2.263790	1.3782
3.0416	1.043216	−2.269784	1.3977
3.5649	0.976629	−2.273091	1.4180
4.1684	0.884006	−2.278657	1.4444
4.6588	0.779136	−2.278012	1.4726
4.9283	0.687550	−2.279063	1.4932
4.9783	0.653526	−2.278331	1.4998
4.9583	0.597939	−2.285583	1.5107
4.9383	0.590097	−2.285532	1.5125
4.8841	0.571555	−2.286078	1.5164
4.6672	0.530166	−2.297245	1.5253
4.2110	0.494560	−2.305207	1.5405
3.7725	0.479436	−2.314343	1.5564
3.3839	0.473571	−2.325197	1.5720
3.1788	0.472891	−2.328132	1.5808
2.8810	0.478773	−2.332380	1.5963
2.6773	0.482944	−2.342306	1.6062

$\gamma = 0.81286$; Figure 5, Curve D.

T	F_i	F_f	x
9.3154	1.100000	−1.454615	1.8458
9.3654	0.974253	−1.561145	1.8426
9.4473	0.848505	−1.658802	1.8391

T	F_i	F_f	x
9.5017	0.772912	-1.716456	1.8349
9.5392	0.703764	-1.771176	1.8270
9.4656	0.612785	-1.870668	1.7928

$\gamma = 0.8172$; Figure 5, Curve D.

9.5284	0.685022	-1.796535	1.8251
9.5216	0.670142	-1.811267	1.8203
9.5020	0.651952	-1.833297	1.8123
9.4802	0.642911	-1.847640	1.8059
8.9262	0.682953	-1.971430	1.7144
8.1661	0.869246	-2.036118	1.6017
7.2142	1.100000	-2.076066	1.4508
6.4838	1.248111	-2.088150	1.3489
5.5995	1.398920	-2.086873	1.2515
4.6398	1.545740	-2.066138	1.1712
4.0747	1.633377	-2.039764	1.1330
3.4589	1.743602	-1.985500	1.0976
3.4142	1.752035	-1.980728	1.0956
3.3858	1.760052	-1.976228	1.0938
3.3436	1.772975	-1.968278	1.0910
3.3034	1.785107	-1.959996	1.0887
3.2605	1.801408	-1.948052	1.0860
3.1790	1.834270	-1.920858	1.0818
3.1490	1.846269	-1.910058	1.0807
3.1190	1.858269	-1.899011	1.0799
3.0890	1.870268	-1.887859	1.0793
3.0590	1.882268	-1.876189	1.0790
3.0252	1.887780	-1.870675	1.0789
3.0092	1.873644	-1.884488	1.0788

$\gamma = +9/11$; Figure 5, Curve D.

** These values are from G. Shearing (2).

12.8316	-0.982968	-1.206407	1.0374
11.911	-0.768	-1.261	**
10.8116	-0.503955	-1.316638	1.3916
10.316	-0.356	-1.389	**
10.178	-0.305	-1.425	**
10.071	-0.260	-1.465	**
9.9860	-0.211202	-1.516090	1.6614
9.8843	0.014507	-1.793023	1.7764
9.6977	0.107176	-1.880600	1.7674
9.5877	0.137872	-1.908034	1.7583
9.4634	0.163567	-1.934719	1.7474
9.0634	0.210409	-1.996508	1.7137
8.8634	0.221359	-2.019785	1.6985
8.0634	0.234541	-2.095893	1.6501
7.0639	0.233863	-2.159491	1.6139
5.2639	0.231625	-2.236989	1.5944
4.4639	0.232667	-2.261660	1.6008

$\gamma = 0.93$; Figure 5, Curve G.

T	F_i	F_f	x
12.2032	-0.857610	-1.016071	1.4843
12.0505	-0.798859	-1.037212	1.5278
11.9590	-0.767233	-1.045792	1.5555
11.1645	-0.496969	-1.100770	1.8702
10.5696	-0.249175	-1.251698	2.1628
10.2673	-0.119823	-1.434482	2.1882
10.1652	-0.084483	-1.497868	2.1696
10.0558	-0.052932	-1.558567	2.1445
10.0014	-0.039471	-1.585843	2.1313
9.8335	-0.005561	-1.657842	2.0920
9.7548	0.006970	-1.686566	2.0745
9.6220	0.024677	-1.729425	2.0470
9.4763	0.040033	-1.769262	2.0194
9.4034	0.046433	-1.788335	2.0064
9.2942	0.054890	-1.813548	1.9884

$F = 0.0$ (ejection); Figure 1, Curve C.

T	γ	F_f	x
3.0109	-0.998423	-2.290942	0.8808
3.7308	-0.895403	-2.266930	0.9041
4.6903	-0.752500	-2.241069	0.9395
5.6503	-0.603080	-2.208723	0.9812
6.6103	-0.445485	-2.171838	1.0314
7.5703	-0.277972	-2.133872	1.0942
8.5295	-0.097404	-2.089977	1.1765
9.4900	0.100000	-2.033354	1.2938
9.9200	0.200000	-2.005400	1.3662
10.6100	0.400000	-1.942935	1.5442
10.6520	0.500000	-1.911453	1.6046
10.4470	0.600000	-1.879996	1.6297
10.1853	0.700000	-1.841121	1.6689
9.9359	0.800000	-1.789348	1.7514
9.7881	0.900000	-1.708553	1.9538
9.8789	0.960000	-1.612897	2.3235
10.0200	0.980000	-1.545998	2.6788
10.4261	0.998000	-1.358174	4.3344

$F = 0.4$; Figure 1, Curve B.

1.3207	-0.961267	-2.268597	1.0882
2.2207	-0.891189	-2.264207	1.0865
2.8207	-0.837714	-2.257711	1.0883
3.4207	-0.778631	-2.249771	1.0926
4.0207	-0.713870	-2.242632	1.0994
4.6204	-0.642881	-2.224948	1.1090
5.2204	-0.565000	-2.211452	1.1218
5.8204	-0.479601	-2.192095	1.1382
6.4204	-0.385658	-2.169883	1.1590
7.0204	-0.281718	-2.142075	1.1856

T	γ	F_f	x
7.6204	− 0.165722	− 2.112189	1.2197
8.2200	− 0.034233	− 2.073859	1.2649
8.8196	0.119183	− 2.027520	1.3278
9.4196	0.310535	− 1.966661	1.4255
9.8196	0.489388	− 1.908368	1.5421
9.9196	0.555991	− 1.888443	1.5931
9.9771	0.614458	− 1.873535	1.6412
9.9921	0.643801	− 1.868223	1.6663
9.9945	0.667903	− 1.865554	1.6871
9.9567	0.717815	− 1.868341	1.7285
9.9067	0.739247	− 1.876710	1.7431
9.7767	0.764976	− 1.901823	1.7520

$F = 1.1$; Figure 1, Curve A.

5.1155	0.000000	− 1.846254	1.1689
6.0154	0.169427	− 1.779875	1.2265
7.0154	0.363733	− 1.696574	1.3197
8.0154	0.560695	− 1.599621	1.4654
9.0154	0.754787	− 1.486356	1.7229
9.3154	0.812860	− 1.454616	1.8458
9.5154	0.855546	− 1.450125	1.9499
9.5434	0.863300	− 1.456104	1.9665
9.5674	0.872343	− 1.469420	1.9813
9.5730	0.879598	− 1.489789	1.9851
9.5133	0.888155	− 1.556001	1.9510
9.4138	0.890214	− 1.617957	1.8990
9.2138	0.887892	− 1.708497	1.8117
8.8138	0.877280	− 1.832627	1.6849
8.0142	0.849129	− 1.983305	1.5345
7.0142	0.809007	− 2.092332	1.4361
6.0243	0.766818	− 2.162782	1.3859
5.0244	0.723883	− 2.208636	1.3633
4.0244	0.682582	− 2.237100	1.3600
3.0244	0.645542	− 2.261210	1.3708
2.5662	0.631454	− 2.264146	1.3795

Class (n)

Initial Conditions: $F_i = 0$; $\dot{E}_i = 0$; $\dot{F}_i > 0$.

Final Conditions: $F_f = 0$; $\dot{E}_f = 0$; $\dot{F}_f < 0$.

Note: To obtain the remainder of the class take the mirror images, i.e. the values

$$E_i' = -E_f;\; E_f' = -E_i.$$

$\gamma = 0$; Figure 6, Curve l

(Use both $E_i' = -E_f$ and $E_i' = 2\pi - E_f$).

T	E_i	E_f	x
7.4904	0.400000	6.210934	1.2311
7.6375	0.350000	6.137804	1.2352
6.9804	− 0.100000	5.789594	1.2189
6.6166	− 0.200000	5.744591	1.2117
6.2229	− 0.300000	5.703364	1.2053
5.3891	− 0.500000	5.626134	1.1957
4.1422	− 0.800000	5.509205	1.1900
3.3838	− 1.000000	5.422646	1.1911
2.7283	− 1.200000	5.323286	1.1945
2.2108	− 1.400000	5.205328	1.1987
1.7361	− 1.800000	4.941247	1.2018
2.0270	− 2.000000	4.635106	1.2004
2.8329	− 2.200000	4.307012	1.1937
4.4679	− 2.400000	3.861233	1.1905
6.5895	− 2.600000	3.348746	1.2112
7.6550	− 2.800000	2.984999	1.2357
7.2995	− 3.141519	2.699071	1.2262

$\gamma = 0.12$; Figure 6, Curve L

(Use both $E_i' = 2\pi - E_f$ and $E_i' = 2\pi + E_i$).

7.1414	0.450000	6.489635	1.2533
8.0077	0.300000	6.192347	1.2772
8.1171	0.200000	6.074334	1.2809
8.0896	0.150000	6.028181	1.2800
7.9879	0.800000	5.975770	1.2766
7.8062	0.000000	5.926997	1.2709
7.5111	− 0.100000	5.877249	1.2625
5.5590	− 0.600000	5.707140	1.2279
4.7490	− 0.800000	5.651921	1.2213
3.3438	− 1.200000	5.548738	1.2151
2.8133	− 1.400000	5.504939	1.2123
2.4414	− 1.600000	5.475323	1.2078
2.2796	− 1.800000	5.471971	1.2015
2.4220	− 2.000000	5.506731	1.1954
3.0267	− 2.200000	5.582736	1.1951
4.2230	− 2.400000	5.690771	1.2087
5.6067	− 2.600000	5.806805	1.2338
6.0650	− 2.700000	5.853539	1.2425
6.2987	− 2.800000	5.883134	1.2459
6.2389	− 3.000000	5.883704	1.2404
6.2223	− 3.010000	5.882064	1.2400
6.2047	− 3.020000	5.880462	1.2393
6.1461	− 3.050000	5.874843	1.2375
6.0309	− 3.100000	5.864022	1.2345
5.7460	− 3.200000	5.838801	1.2280
5.0249	− 3.400000	5.782592	1.2157
4.1922	− 3.600000	5.724087	1.2063
3.3228	− 3.800000	5.663149	1.2009
2.4700	− 4.000000	5.597251	1.1989
1.6746	− 4.200000	5.523654	1.1997
0.9707	− 4.400000	5.438039	1.2021

T	E_i	E_f	x
0.3913	−4.600000	5.335028	1.2051
−0.0224	−4.800000	5.206345	1.2076
−0.2046	−5.000000	5.037020	1.2089

$\gamma = 0.12$; Figure 6, Curve M
(Use $E_i' = -E_f$).

T	E_i	E_f	x
7.3999	−2.800000	2.851901	1.2076
7.3865	−2.700000	2.699355	1.2157
7.0904	−2.650000	3.044587	1.2001
6.8597	−2.600000	3.126193	1.1952
5.3940	−2.400000	3.512190	1.1753
3.9553	−2.200000	3.856758	1.1738
3.1750	−2.000000	4.067730	1.1832
2.9466	−1.800000	4.155876	1.1923
3.0880	−1.600000	4.149906	1.1964
3.4812	−1.400000	4.077415	1.1937
4.0549	−1.200000	3.962671	1.1847
4.7694	−1.000000	3.819245	1.1718
5.1700	−0.900000	3.739651	1.1650
6.0408	−0.700000	3.567682	1.1532
7.0755	−0.480000	3.360621	1.1478
8.0109	−0.288000	3.162184	1.1548
8.9530	−0.096000	2.930121	1.1808
9.1933	−0.048000	2.857031	1.1924
9.3170	−0.024000	2.814142	1.1996
9.3600	−0.016000	2.797344	1.2024
9.4030	−0.008000	2.780304	1.2053
9.4488	0.000000	2.759620	1.2087
9.5000	0.008475	2.733884	1.2128
9.5600	0.016750	2.695403	1.2183
9.5980	0.010000	2.610246	1.2259
9.5525	−0.010000	2.567793	1.2260
9.0512	−0.160000	2.428853	1.2075
8.7462	−0.240000	2.395199	1.1953
7.0000	−0.713935	2.172098	1.1584
6.7277	−0.800000	2.127035	1.1569
6.4403	−0.900000	2.072618	1.1567
6.1916	−1.000000	2.011915	1.1580
5.8191	−1.200000	1.875669	1.1637
5.6225	−1.400000	1.712284	1.1699
5.5855	−1.600000	1.518725	1.1717

$\gamma = 0.12$; Figure 6, Curve U (Use $E_i' = -E_f$);
Figure 7, Curve C (Use $E_i' = -2\pi - E_f$).

T	E_i	E_f	x
14.3000	−1.642525	−1.392107	1.1074
12.7000	−1.721351	−1.305757	1.1221
11.1000	−1.825580	−1.195419	1.1408
10.3000	−1.904260	−1.116336	1.1553
9.9000	−1.961563	−1.060986	1.1668
9.7000	−2.001575	−1.023372	1.1756
9.6000	−2.028246	−0.998807	1.1820
9.5000	−2.066648	−0.964194	1.1920
9.4530	−2.100000	−0.934840	1.2015
9.5106	−2.200000	−0.851364	1.2357
9.7933	−2.300000	−0.777255	1.2770
10.1280	−2.400000	−0.718086	1.3145
10.3087	−2.500000	−0.677854	1.3273
10.2875	−2.600000	−0.653942	1.3124
10.1332	−2.700000	−0.643149	1.2850
9.8986	−2.800000	−0.643004	1.2552
9.6092	−2.900000	−0.650603	1.2266
9.2788	−3.000000	−0.663607	1.2007
8.7591	−3.141593	−0.688494	1.1688
7.3021	−3.500000	−0.776222	1.1127
5.4075	−4.000000	−0.964106	1.0822
4.4350	−4.400000	−1.196724	1.0841
4.2000	−4.600000	−1.350747	1.0878
4.1373	−4.800000	−1.537870	1.0892

$\gamma = 0.664928$; Figure 6, Curve m
(Use $E_i' = -E_f$).

T	E_i	E_f	x
8.5085	−1.435203	1.435164	1.5794
8.5600	−1.363739	1.465832	1.5818
8.5614	−1.326323	1.504190	1.5800
8.5694	−1.207676	1.635203	1.5672
8.6059	−1.075760	1.800000	1.5420
8.6240	−1.035203	1.858883	1.5316
8.6291	−1.025203	1.873969	1.5290
8.6332	−1.015203	1.890972	1.5259
8.6360	−1.009540	1.900000	1.5242
8.6531	−0.959896	2.000000	1.5057
8.6516	−0.947887	2.035203	1.4991
8.5217	−0.942244	2.235203	1.4614
8.1174	−1.077353	2.435203	1.4239
7.9450	−1.155001	2.490292	1.4120
7.8070	−1.227486	2.527287	1.4020
7.7040	−1.290054	2.550713	1.3936
7.6022	−1.362765	2.569325	1.3838
7.5009	−1.454143	2.581338	1.3711
7.4262	−1.549150	2.581094	1.3575
7.3700	−1.744775	2.541089	1.3304
7.3752	−1.794775	2.521817	1.3242
7.3870	−1.844775	2.498892	1.3186
7.3982	−1.878979	2.481094	1.3151
7.4204	−1.933978	2.449013	1.3101
7.4414	−1.981094	2.418251	1.3064
7.4643	−2.031094	2.381695	1.3033
7.4858	−2.081094	2.340979	1.3011

T	E_i	E_f	x
7.5014	−2.131094	2.299125	1.2992
7.5111	−2.181094	2.253458	1.2982
7.5156	−2.200698	2.231094	1.2987

$\gamma = 0.90$; Figure 7, Curve B
(Use $E'_i = -2\pi - E_f$).

12.6651	−1.063722	−0.938363	1.7594
11.8651	−1.126858	−0.789508	1.8340
11.0651	−1.226252	−0.621978	1.9204
10.9260	−1.257893	−0.587648	1.9321
10.6851	−1.333829	−0.524094	1.9408
10.5260	−1.403931	−0.480583	1.9320
10.2271	−1.579706	−0.405808	1.8707
10.1260	−1.644840	−0.385742	1.8403
9.8271	−1.824019	−0.343221	1.7490
9.7260	−1.877760	−0.333016	1.7211
9.4271	−2.018918	−0.311357	1.6488
9.3260	−2.061620	−0.305983	1.6275
9.0271	−2.176877	−0.293845	1.5720
8.9260	−2.212732	−0.290678	1.5553
8.5260	−2.343195	−0.281658	1.4974
7.8271	−2.540325	−0.274153	1.4184
7.4271	−2.641436	−0.272740	1.3819
7.0271	−2.736668	−0.272701	1.3499
6.6271	−2.827397	−0.273756	1.3215
6.1283	−2.935767	−0.276555	1.2902
5.4296	−3.081329	−0.282402	1.2526
5.0300	−3.162400	−0.286952	1.2335
4.2312	−3.321993	−0.298363	1.1998
3.4321	−3.481125	−0.313283	1.1708
2.6321	−3.643197	−0.332578	1.1454
1.8321	−3.811608	−0.358016	1.1226
1.4321	−3.899522	−0.373927	1.1120
0.6321	−4.086330	−0.414716	1.0914
−0.1679	−4.294916	−0.474997	1.0704
−0.5679	−4.411633	−0.516691	1.0593
−0.9679	−4.541022	−0.571788	1.0473
−1.3679	−4.690478	−0.647886	1.0341
−1.7679	−4.880737	−0.766572	1.0193

$E = 0.0$ (ejection); Figure 1, Curve D.

T	γ	E_f	x
4.7134	−0.980000	3.014695	1.5058
5.7470	−0.780000	2.726271	1.1444
6.9160	−0.540000	2.572900	1.1073
8.0045	−0.300000	2.484056	1.1304
9.0333	−0.050000	2.454016	1.1873
9.3934	0.050000	2.484227	1.2146
9.5433	0.100000	2.532928	1.2257
9.5780	0.120000	2.585546	1.2263
9.5777	0.124352	2.607312	1.2253
9.4000	0.113687	2.794480	1.2040
9.2000	0.082986	2.914247	1.1881
8.9516	0.040000	3.039766	1.1737
8.1025	−0.120000	3.410892	1.1563
6.8726	−0.360000	3.972052	1.2024
6.1010	−0.480000	4.530340	1.2436
5.9000	−0.486756	4.780068	1.2302
5.8500	−0.482016	4.871404	1.2213
5.8010	−0.454000	5.081769	1.1982
5.8097	−0.440000	5.145236	1.1914
5.8747	−0.400000	5.281857	1.1792
5.9729	−0.360000	5.382432	1.1733
6.0900	−0.320000	5.463298	1.1714
6.3587	−0.240000	5.590714	1.1751
6.9713	−0.080000	5.772051	1.2035
7.9777	0.160000	5.952280	1.2889
8.6677	0.320000	6.526296	1.3800
9.9733	0.640000	6.384434	1.7252
10.2330	0.720000	6.273174	1.8865
10.2800	0.735000	6.282122	1.9221
10.3400	0.754223	6.319649	1.9707
10.4480	0.801742	6.275482	2.1161
10.5200	0.854592	6.283663	2.3259

Class (α-δ)

Initial Conditions:

$$E_i = 0;\ \dot{F}_i = 0;\ \dot{E}_i > 0.$$

Final Conditions:

$$E_f = 0;\ \dot{F}_f = 0;\ \dot{E}_f > 0\ \ (\alpha\text{-symmetry});$$
$$E_f = 0;\ \dot{F}_f = 0;\ \dot{E}_f < 0\ \ (\delta\text{-symmetry}).$$

Note: To obtain the remainder of the class take the mirror images, i.e. the values

$$F'_i = F_f;\quad F'_f = F_i\ \ (\alpha\text{-symmetry});$$
$$F'_i = -F_f;\ F'_f = -F_i\ \ (\delta\text{-symmetry}).$$

$\gamma = -0.709554$ (δ-symmetry); Figure 8, Curve S.

T	F_i	F_f	x
10.5687	−1.015411	0.997742	2.0200
10.5061	−1.009873	0.976199	2.0249
10.4515	−1.005338	0.956381	2.0299
10.3627	−0.999615	0.920149	2.0399
10.2627	−0.983760	0.891637	2.0499
10.0627	−0.949578	0.836697	2.0714
9.5634	−0.864226	0.690083	2.1404
9.0962	−0.784583	0.531643	2.2292
8.5518	−0.683320	0.325575	2.3597

T	F_i	F_f	x
8.1057	– 0.577810	0.189289	2.4592
7.8931	– 0.518200	0.138729	2.5034
7.6760	– 0.448669	0.096033	2.5489
7.5532	– 0.403563	0.077262	2.5757
7.3285	– 0.303030	0.055748	2.6296
7.2588	– 0.263030	0.055278	2.6489
7.1893	– 0.211362	0.065929	2.6690
7.1736	– 0.198116	0.069233	2.6740
7.1489	– 0.172686	0.078875	2.6820
7.1349	– 0.151677	0.091086	2.6866
7.1288	– 0.140998	0.097702	2.6886
7.1218	– 0.130006	0.103659	2.6911
7.1158	– 0.120731	0.108445	2.6932
7.0912	– 0.098140	0.111898	2.7020
7.0743	– 0.096512	0.100119	2.7083

$\gamma = -0.689294$ (α, δ-symmetries); Figure 8, Curve B.
* These orbits have the δ-symmetry.

13.3393	– 1.144866	1.258549	1.7732*
13.2044	– 0.992640	1.380179	1.7845*
13.1176	– 0.932864	1.420471	1.7913*
13.0218	– 0.877531	1.455232	1.7984*
12.8120	– 0.777013	1.511124	1.8130*
12.5520	– 0.674179	1.561245	1.8294*
12.1040	– 0.527095	1.622150	1.8534
11.0705	– 0.262351	1.702975	1.8885
10.1440	– 0.071756	1.739257	1.8996
9.1747	0.104260	1.750015	1.8974
8.1941	0.270458	1.739746	1.8864
7.1972	0.435419	1.710398	1.8697
6.2078	0.602989	1.660566	1.8505
5.6253	0.708044	1.619940	1.8385
5.0578	0.820380	1.563586	1.8267
4.5202	0.945952	1.489123	1.8155
4.2020	1.042163	1.420886	1.8089
4.0673	1.096018	1.378919	1.8061
3.9599	1.156582	1.327781	1.8039
3.8929	1.236986	1.253377	1.8028

$\gamma = -0.545909$ (α, δ-symmetries);
Figures 8 and 9, Curve P.
* These orbits have the δ-symmetry.

T	F_i	F_f	x
13.1541	– 1.226468	1.219245	1.8540*
13.1421	– 1.186604	1.259490	1.8580*
13.1302	– 1.146771	1.292707	1.8654*
13.1242	– 1.126771	1.307234	1.8703*
13.1042	– 1.077385	1.339661	1.8864*
13.0586	– 0.986821	1.387106	1.9271*
13.0338	– 0.942908	1.405792	1.9515*
12.9903	– 0.869885	1.432362	1.9980*
12.9518	– 0.804530	1.451827	2.0445*
12.9221	– 0.749924	1.465664	2.0856*
12.9027	– 0.704801	1.475292	2.1187*
12.8956	– 0.680489	1.479484	2.1353*
12.8928	– 0.641489	1.484583	2.1572*
12.8934	– 0.640493	1.484584	2.1575*
12.8944	– 0.631348	1.485526	2.1616*
12.8968	– 0.621348	1.486188	2.1653*
12.9037	– 0.602344	1.487342	2.1706*
12.9090	– 0.591475	1.487949	2.1726*
12.9209	– 0.571475	1.489097	2.1739*
12.9275	– 0.560869	1.489895	2.1738*
12.9399	– 0.542583	1.491536	2.1716*
12.9416	– 0.540160	1.491787	2.1711*
12.9632	– 0.453738	1.512620	2.1450*
12.9579	– 0.441583	1.517388	2.1405*
12.9480	– 0.426365	1.523160	2.1348*
12.9364	– 0.413352	1.528551	2.1299*
12.9089	– 0.390334	1.539186	2.1214*
12.7759	– 0.322355	1.571951	2.0973
12.0000	– 0.126940	1.663449	2.0395
11.1136	0.020110	1.711224	2.0042
10.0226	0.175354	1.734588	1.9709
9.0665	0.306546	1.732106	1.9448
8.1170	0.440490	1.710000	1.9200
7.0234	0.606733	1.653668	1.8930
6.1089	0.765279	1.577660	1.8721
5.2592	0.953912	1.456968	1.8546
5.0208	1.027980	1.399724	1.8502
4.9203	1.067464	1.367219	1.8484
4.8380	1.108000	1.332327	1.8469
4.7410	1.188852	1.258154	1.8454
4.6994	1.227786	1.223642	1.8467
4.6843	1.226078	1.227146	1.8474

$\gamma = -0.541909$ (δ-symmetry); Figure 9, Curve R.

12.6441	– 1.328566	1.302708	1.9212
12.6322	– 0.917286	1.5208	2.1358
12.6427	– 0.814040	1.540175	2.2122
12.6598	– 0.719644	1.549052	2.2705
12.6707	– 0.671727	1.550130	2.2945
12.6761	– 0.627689	1.552055	2.3198
12.6715	– 0.598737	1.556572	2.3450
12.6515	– 0.550943	1.569658	2.4046
12.6313	– 0.509312	1.580651	2.4666
12.6090	– 0.459056	1.581382	2.5270
12.5196	– 0.362922	1.537900	2.5616

T	F_i	F_f	x
12.4479	−0.324802	1.509771	2.5591
12.2218	−0.246823	1.441627	2.5474
11.9208	−0.175196	1.369275	2.5373
11.5646	−0.108134	1.295038	2.5319
11.0937	−0.033526	1.204861	2.5317
10.2949	−0.074784	1.058640	2.5439
9.2855	0.195242	0.868301	2.5799
8.7095	0.258885	0.748303	2.6139
8.2420	0.307705	0.637375	2.6534
7.9205	0.339041	0.547809	2.6911
7.7133	0.357481	0.479200	2.7235
7.5535	0.369882	0.415432	2.7565
7.4576	0.375996	0.368399	2.7824
7.4038	0.378513	0.336899	2.8005
7.3007	0.379622	0.253043	2.8509
7.2614	0.375877	0.196331	2.8859
7.2200	0.354974	0.025841	2.9857
7.1834	0.346139	−0.059647	3.0251
7.1024	0.341457	−0.143863	3.0533
7.0084	0.336697	−0.210352	3.0676
6.9430	0.330034	−0.253016	3.0735
6.9052	0.319254	−0.282948	3.0759
6.8872	0.308620	−0.302462	3.0767
6.8643	0.311390	−0.311359	3.0770

$\gamma = -0.518320$ (α, δ-symmetries);
Figures 9 and 10, Curve M.
* These orbits have the δ-symmetry.

12.0000	−0.080573	1.665048	2.0522
12.0988	−0.098139	1.658339	2.0580
12.2092	−0.118596	1.649003	2.0650
12.3057	−0.137390	1.640204	2.0717
12.5402	−0.187862	1.615458	2.0917
12.7171	−0.233289	1.591364	2.1128
12.8617	−0.280513	1.565375	2.1395
12.9509	−0.323344	1.540498	2.1712*
12.9822	−0.356868	1.522683	2.2064*
12.9731	−0.377039	1.514492	2.2388*
12.9500	−0.387360	1.512598	2.2654*
12.9470	−0.388166	1.512636	2.2683*
12.8218	−0.395622	1.535948	2.3727*
12.7552	−0.388669	1.562407	2.4462*
12.7012	−0.374123	1.594808	2.5610*
12.6806	−0.353091	1.594051	2.6174*
12.6519	−0.326155	1.572616	2.6200*
12.6095	−0.300679	1.548582	2.6110*
12.5022	−0.257219	1.504765	2.5929*
12.2873	−0.196957	1.440558	2.5712*
12.0000	−0.135805	1.371946	2.5558*

$\gamma = -0.518320$ (α-symmetry);
Figures 9 and 10, Curve N.

T	F_i	F_f	x
11.9132	−0.120780	1.846227	2.9980
12.2255	−0.190911	1.801823	3.0039
12.5173	−0.264921	1.748547	3.0226
12.6111	−0.305719	1.715661	3.0365
12.6388	−0.323051	1.701104	3.0411
12.6523	−0.333997	1.691637	3.0423
12.6717	−0.359235	1.669743	3.0227
12.6767	−0.379131	1.653404	2.8711
12.6768	−0.395000	1.651277	2.7603
12.6497	−0.445000	1.674778	2.7338
12.6239	−0.505000	1.688753	2.7195
12.6272	−0.565000	1.687732	2.6842
12.6375	−0.608614	1.683277	2.6544
12.6470	−0.648252	1.678834	2.6296
12.6585	−0.728277	1.674157	2.5980
12.6592	−0.782292	1.676177	2.5894
12.6549	−0.834230	1.681720	2.5786
12.6452	−0.891963	1.689910	2.5566
12.6156	−0.991782	1.706798	2.5019
12.5836	−0.058482	1.719953	2.4633
12.5464	−1.110511	1.732222	2.4355
12.4505	−1.183259	1.757105	2.4026
12.2643	−1.218700	1.791760	2.3883
12.1737	−1.215910	1.805310	2.3880
11.9215	−1.185863	1.836490	2.3952
11.4243	−1.099591	1.881127	2.4293
10.8481	−0.989794	1.919059	2.4925

$\gamma = -0.514645$ (δ-symmetry);
Figure 9, Curve M.

13.0428	−1.260716	1.245300	1.8691
13.0328	−1.240716	1.268995	1.8708
13.0178	−1.210716	1.300218	1.8761
13.0077	−1.191143	1.318348	1.8813
12.9911	−1.160166	1.344111	1.8918
12.9735	−1.131611	1.365792	1.9042
12.9541	−1.109170	1.383090	1.9167
12.9361	−1.087775	1.398185	1.9299
12.9121	−1.070610	1.412857	1.9440
12.8521	−1.055174	1.438532	1.9704
12.8253	−1.075138	1.440431	1.9692
12.8106	−1.124583	1.424644	1.9491
12.8053	−1.211137	1.378000	1.9153
12.8055	−1.292869	1.312722	1.8995

$\gamma = -0.483940$ (α, δ-symmetries);
Figures 9 and 10, Curve LH.
* These orbits have the δ-symmetry.

T	F_i	F_f	x
12.0000	−0.031021	1.667418	2.0636
12.4870	−0.116894	1.628215	2.1010
12.8979	−0.214332	1.571051	2.1665
13.0115	−0.260907	1.540038	2.2248*
13.0220	−0.278291	1.528901	2.2656*
12.9939	−0.288430	1.526034	2.3179*
12.9667	−0.290123	1.529124	2.3487*
12.9087	−0.288642	1.543013	2.4091*
12.8195	−0.280895	1.585049	2.5433*
12.7862	−0.279537	1.621512	2.6891*
12.7657	−0.290874	1.652301	2.7564
12.7086	−0.300834	1.685080	2.8108
12.5972	−0.304460	1.719896	2.8771
12.4911	−0.302788	1.742340	2.9269
12.2410	−0.295594	1.780708	3.0230
12.1073	−0.294217	1.796148	3.0664
12.0188	−0.296120	1.805378	3.0922
11.9017	−0.307369	1.817201	3.1207
11.8636	−0.317978	1.820000	3.1262
11.8430	−0.335676	1.822141	3.1230
11.8504	−0.355575	1.821076	3.1107
11.9522	−0.413576	1.811935	3.0508
12.1682	−0.493064	1.790155	2.9407
12.4358	−0.590206	1.752899	2.7896
12.6591	−0.717019	1.705199	2.6129
12.7220	−0.801695	1.684268	2.5345
12.7419	−0.895644	1.678139	2.4943
12.7414	−0.921505	1.679581	2.4879
12.7251	−1.009512	1.691251	2.4618
12.6884	−1.092472	1.707923	2.4284
12.6326	−1.160978	1.726689	2.4015
12.5572	−1.209532	1.745852	2.3861
12.4471	−1.236646	1.768521	2.3796
12.3971	−1.239751	1.777150	2.3791
12.2863	−1.236085	1.794281	2.3804
12.0903	−1.212812	1.818612	2.3871
11.5102	−1.113049	1.871494	2.4277
10.9277	−1.003846	1.908916	2.4923
10.3441	−0.889090	1.939062	2.5793
9.7794	−0.768793	1.959884	2.6893
9.4208	−0.683388	1.972676	2.7788
9.1714	−0.615862	1.978454	2.8571
8.9000	−0.523380	1.983139	2.9801
8.8548	−0.501989	1.981062	3.0132
8.8238	−0.482692	1.980092	3.0464
8.8090	−0.460163	1.977263	3.0931
8.9000	−0.443329	1.967329	3.1736
9.0022	−0.449767	1.960540	3.2060
9.1145	−0.461707	1.953631	3.2305
9.5836	−0.524484	1.930537	3.3025
10.1655	−0.604076	1.901709	3.3961
10.7896	−0.685088	1.869574	3.5691

$\gamma = -0.483940$ (δ-symmetry);
Figures 9 and 10, Curve Q.

6.7472	0.410600	−0.417778	3.1160
6.7563	0.401533	−0.423472	3.1161
6.7625	0.397774	−0.424768	3.1162
6.8543	0.354155	−0.433774	3.1167
7.1097	0.254085	−0.426462	3.1132
7.3048	0.155542	−0.415843	3.0974
7.4068	0.051444	−0.412554	3.0630
7.4199	−0.011348	−0.415764	3.0331
7.4016	−0.112817	−0.426542	2.9736
7.3940	−0.159421	−0.432036	2.9434
7.3948	−0.195717	−0.435794	2.9194
7.4014	−0.224738	−0.438220	2.9002
7.4393	−0.287866	−0.440769	2.8590
7.4915	−0.335161	−0.439745	2.8292
7.6702	−0.434010	−0.429152	2.7714
7.8791	−0.513283	−0.412200	2.7300
8.1481	−0.594525	−0.387488	2.6923
8.4578	−0.673832	−0.357385	2.6602
8.9708	−0.787530	−0.304605	2.6217
9.7082	−0.931100	−0.224907	2.5855
10.2922	−1.036621	−0.158682	2.5679
11.0764	−1.175285	−0.062558	2.5574
11.6520	−1.280914	+0.016846	2.5613
12.1274	−1.377736	0.093187	2.5778
12.4201	−1.448271	0.150170	2.6007
12.6914	−1.539940	0.221624	2.6520
12.7503	−1.574239	0.245942	2.6813
12.7658	−1.588197	0.254963	2.6961
12.7801	−1.617334	0.270626	2.7489
12.7786	−1.628212	0.273143	2.8126
12.7761	−1.640212	0.274472	3.0037

$\gamma = -0.402450$ (α, δ-symmetries);
Figure 9, Curve K.
* These orbits have the δ-symmetry.

5.5035	1.194047	1.212530	1.8973
5.5537	1.128715	1.274883	1.8976
5.6521	1.067702	1.331237	1.8990
5.8206	1.000000	1.389986	1.9017
6.2206	0.889123	1.476414	1.9088

T	F_i	F_f	x
6.9748	0.738316	1.575849	1.9243
7.7276	0.616857	1.638643	1.9417
8.4982	0.507605	1.680006	1.9607
9.2982	0.403644	1.703918	1.9816
10.0982	0.304627	1.711521	2.0041
10.8982	0.206217	1.704287	2.0302
11.6982	0.103203	1.681663	2.0642
12.2982	0.017749	1.650112	2.1023
12.6982	−0.047694	1.617068	2.1437
12.8982	−0.085615	1.594124	2.1777
13.0980	−0.132970	1.559771	2.2481
13.1209	−0.140576	1.553786	2.2671
13.1383	−0.148294	1.547770	2.2930*
13.1297	−0.158611	1.543743	2.3726*
13.1157	−0.159259	1.546821	2.3996*
13.0688	−0.158006	1.563331	2.4810*
13.0177	−0.155991	1.598091	2.6154*
13.0085	−0.156206	1.608008	2.6541*
12.9680	−0.158001	1.645103	2.7729
12.8972	−0.155422	1.676986	2.8494
12.1593	−0.088122	1.792171	3.1590
11.5232	−0.038884	1.838876	3.3415
11.0618	−0.016199	1.862292	3.4700
10.8596	−0.012094	1.871018	3.5304
10.6359	−0.014844	1.879485	3.6064
10.5437	−0.019238	1.882540	3.6447
10.3947	−0.200178	1.886008	3.6938
10.4580	−0.212234	1.885124	3.6163
10.5170	−0.233603	1.883274	3.5730
10.7241	−0.303787	1.877200	3.4571
11.0281	−0.390329	1.864975	3.3216
11.4580	−0.496179	1.842338	3.1519
11.9152	−0.600707	1.812613	2.9754
12.3674	−0.707461	1.771777	2.7836
12.5762	−0.765637	1.745954	2.6783
12.7948	−0.853123	1.708413	2.5383
12.9107	−0.956928	1.679184	2.4310
12.9287	−1.002472	1.674214	2.4067
12.9336	−1.049722	1.674175	2.3919
12.9238	−1.106634	1.680310	2.3807
12.9031	−1.152981	1.688927	2.3727
12.8102	−1.240729	1.716964	2.3625
12.7281	−1.266865	1.735047	2.3641
12.6462	−1.273220	1.749938	2.3679
12.5421	−1.268107	1.766157	2.3732
12.0997	−1.202232	1.816827	2.4007
11.3489	−1.068415	1.870943	2.4729
10.6177	−0.933358	1.908203	2.5744

T	F_i	F_f	x
10.1038	−0.832535	1.928617	2.6667
9.4988	−0.699968	1.947896	2.8086
9.2147	−0.626873	1.955935	2.8978
8.9767	−0.551757	1.959514	3.0020
8.8611	−0.494045	1.956965	3.1038
8.8591	−0.491372	1.955971	3.1100
8.8574	−0.487380	1.957103	3.1199

$\gamma = 0.0$ (α-symmetry); Figure 8, Curve C.

T	F_i	F_f	x
10.3981	−0.402676	1.774956	3.8053
10.6322	−0.462076	1.771767	3.6214
10.8911	−0.519029	1.765072	3.4964
11.2416	−0.587389	1.754880	3.3575
11.8268	−0.690430	1.733793	3.1530
12.4458	−0.792389	1.705468	2.9410
13.0550	−0.893299	1.664336	2.7058
13.3370	−0.948258	1.636953	2.5728
13.5190	−0.997348	1.613326	2.4701
13.6051	−1.031793	1.599282	2.4149
13.6517	−1.057759	1.590466	2.3836
13.7012	−1.098977	1.579796	2.3517
13.7257	−1.134542	1.574384	2.3409
13.7380	−1.188174	1.572501	2.3495
13.7378	−1.193173	1.572768	2.3515
13.7371	−1.200620	1.573250	2.3549
13.7309	−1.225302	1.575980	2.3686
13.7228	−1.242104	1.579082	2.3801
13.7051	−1.264911	1.584654	2.3996
13.6980	−1.271308	1.586563	2.4062
13.6167	−1.300120	1.605834	2.4586
13.5366	−1.298393	1.620135	2.4874
13.3985	−1.279916	1.640036	2.5167
13.0071	−1.213432	1.679188	2.5682
12.6185	−1.148325	1.706821	2.6151
12.1860	−1.077959	1.730439	2.6726
11.7478	−1.007329	1.750493	2.7387
11.2744	−0.930074	1.768520	2.8203
11.0405	−0.890988	1.775817	2.8652

$\gamma = 0.0$ (δ-symmetry); Figure 8, Curve V.

T	F_i	F_f	x
7.0808	0.782899	−0.784700	3.4022
7.1172	0.766872	−0.785556	3.4045
7.3130	0.704822	−0.785471	3.4121
7.5838	0.640649	−0.764402	3.4226
8.0463	0.540855	−0.719740	3.4423
8.4937	0.446337	−0.673047	3.4630
9.0069	0.332406	−0.618440	3.4891

T	F_i	F_f	x
9.5677	0.176769	−0.558603	3.5176
9.7166	0.101222	−0.542851	3.5179
9.7373	0.070038	−0.540627	3.5120
9.7057	0.022269	−0.544209	3.4933
9.5821	−0.026479	−0.557884	3.4598
9.1421	−0.119740	−0.606359	3.3639
8.7580	−0.200000	−0.650222	3.2735
8.5371	−0.277374	−0.677931	3.1939
8.4918	−0.313301	−0.685149	3.1602
8.4803	−0.353301	−0.688673	3.1248
8.4907	−0.376558	−0.688824	3.1051
8.5535	−0.428186	−0.684640	3.0640
8.7237	−0.501789	−0.668776	3.0106
9.2445	−0.641422	−0.613799	2.9244
9.8355	−0.760004	−0.548411	2.8656
10.5315	−0.880092	−0.470337	2.8193
11.2808	−0.998668	−0.384619	2.7883
12.0669	−1.119571	−0.291343	2.7761
12.8327	−1.243066	−0.193595	2.7955
13.5167	−1.379117	−0.093412	2.9008
13.6146	−1.405678	−0.076351	2.9493
13.7255	−1.444170	−0.053548	3.1210

$\gamma = 0.8609$ (α-symmetry); Figure 8, Curve D.

12.7057	1.123057	0.077541	4.4672
12.6167	1.122501	0.118420	4.1847
12.4468	1.124336	0.183746	4.0209
12.2771	1.123815	0.242552	3.9538
12.1077	1.120725	0.297861	3.9225
11.9406	1.115148	0.350632	3.9108
11.8586	1.111445	0.376239	3.9098
11.6989	1.102230	0.425997	3.9148
11.5475	1.090637	0.473693	3.9265
11.4072	1.076774	0.519062	3.9423
11.2818	1.061033	0.561228	3.9600
11.1691	1.043135	0.601165	3.9782
11.0794	1.025407	0.635191	3.9946
10.9594	0.993913	0.686258	4.0184
10.9007	0.973164	0.715365	4.0309
10.8577	0.953797	0.740269	4.0402
10.8304	0.938576	0.758610	4.0462
10.8031	0.919100	0.780992	4.0523
10.7833	0.900060	0.802147	4.0569
10.7754	0.889537	0.813458	4.0587
10.7685	0.877301	0.826488	4.0604
10.7617	0.864426	0.840885	4.0625
10.7474	0.857602	0.853769	4.0682

$F = -0.641489$ (α, δ-symmetries);
Figure 1, Curve G.
* These orbits have the α-symmetry.

T	γ	F_f	x
10.8100	−0.997198	1.652782	1.5942*
11.2069	−0.890456	1.649245	1.6521*
11.5591	−0.821976	1.639639	1.7011*
12.1515	−0.732938	1.604154	1.7847*
12.5821	−0.670859	1.562585	1.8580
12.9146	−0.607913	1.510220	1.9545
12.9812	−0.585685	1.491823	2.0013
12.9963	−0.574685	1.483261	2.0300
12.9725	−0.556462	1.475352	2.0942
12.9159	−0.547909	1.480728	2.1418
12.8020	−0.541251	1.506366	2.2146
12.7552	−0.540367	1.521351	2.2461
12.7022	−0.540846	1.540895	2.2872
12.6413	−0.544607	1.561800	2.3417
12.6031	−0.549579	1.566386	2.3680
12.5490	−0.558097	1.559565	2.3803
12.4945	−0.566265	1.546779	2.3774
12.3581	−0.583331	1.512277	2.3568
12.0377	−0.612403	1.437931	2.3100
11.5603	−0.641774	1.336789	2.2577
11.1366	−0.660598	1.249886	2.2218
10.5772	−0.679983	1.132564	2.1855
10.1163	−0.693248	1.028360	2.1662
9.5373	−0.707149	0.876529	2.1625
9.1966	−0.713253	0.766624	2.1787
8.9707	−0.716335	0.678247	2.2025
8.7414	−0.716865	0.566493	2.2451
8.6490	−0.716664	0.511382	2.2702
8.5290	−0.715385	0.426008	2.3132
8.4109	−0.712056	0.317821	2.3723
8.3636	−0.709554	0.263808	2.4028
8.3062	−0.704196	0.184724	2.4472
8.2609	−0.695942	0.105139	2.4903
8.2364	−0.688017	0.050163	2.5184
8.2070	−0.667163	−0.047271	2.5632
8.2013	−0.657275	−0.081859	2.5774
8.2008	−0.655922	−0.086104	2.5791

$F = -0.445$ (α-symmetry).
Connection between Curves K and H, Figure 9.

11.2440	−0.402480	1.854045	3.2348
11.2800	−0.408710	1.853222	3.2244
11.3194	−0.415148	1.851806	3.2131
11.3694	−0.422729	1.850843	3.1990
11.4194	−0.429734	1.848178	3.1851
11.4886	−0.438578	1.844922	3.1660

T	γ	F_f	x
11.5600	−0.446782	1.841153	3.1463
11.6336	−0.454383	1.836842	3.1260
11.7094	−0.461400	1.831957	3.1048
11.7874	−0.467844	1.826511	3.0827
11.8672	−0.473730	1.820420	3.0596
11.9489	−0.479086	1.812589	3.0354
12.0322	−0.483943	1.804176	3.0099
12.1322	−0.489080	1.793631	2.9778
12.2890	−0.495984	1.772956	2.9231
12.5239	−0.505963	1.728193	2.8217
12.6039	−0.511330	1.702285	2.7734
12.6453	−0.517075	1.679181	2.7386
12.6558	−0.522320	1.663161	2.7287

$T = 12.6686$ (α-symmetry).

Connection between Curves K and H, Figure 9.

γ	F_i	F_f	x
−0.483942	−0.303300	1.699833	2.8374
−0.481896	−0.297300	1.701180	2.8426
−0.479512	−0.290490	1.702530	2.8485
−0.475364	−0.279084	1.705191	2.8583
−0.471055	−0.267787	1.707349	2.8680
−0.466655	−0.256782	1.709764	2.8774
−0.462193	−0.246123	1.711717	2.8864
−0.457530	−0.235472	1.713828	2.8953
−0.452789	−0.225109	1.715819	2.9040
−0.447923	−0.214926	1.717581	2.9124
−0.442880	−0.204810	1.719690	2.9208
−0.437667	−0.194784	1.721025	2.9291
−0.432293	−0.184867	1.722880	2.9372
−0.426722	−0.174998	1.724318	2.9452
−0.420958	−0.165192	1.725768	2.9531
−0.415986	−0.157040	1.727310	2.9598
−0.410826	−0.148857	1.728110	2.9664
−0.407702	−0.144033	1.728672	2.9702
−0.404631	−0.139381	1.729361	2.9740

Class (g)

Initial Conditions: $F_i = 0;\ \dot{E}_i = 0;\ \dot{F}_i > 0.$

Final Conditions: $E_f = 0;\ \dot{F}_f = 0;\ \dot{E}_f < 0.$

Note: This class is also represented by the conditions

$$E'_i = 0;\ \dot{F}'_i = 0;\ \dot{E}'_i > 0.$$

$$F'_f = 0;\ \dot{E}'_f = 0;\ \dot{F}'_f > 0.$$

To obtain this representation take

$$F'_i = -F_f;\ E'_f = E_i.$$

$\gamma = -0.946809$ (g-symmetry);

Figures 11 and 13, Curve H.

T	E_i	F_f	x
9.4175	−2.880677	−1.960658	3.8095
9.7327	−2.866934	−1.920731	4.0900
10.1012	−2.833244	−1.878231	4.4067
10.4103	−2.784258	−1.841503	4.6904
10.8014	−2.682391	−1.793497	4.8757
11.0000	−2.618061	−1.764439	4.7486
11.0500	−2.601777	−1.755991	4.6923
11.1366	−2.573799	−1.739194	4.5704
11.1793	−2.560041	−1.729620	4.4946
11.2323	−2.542617	−1.715198	4.3686
11.2437	−2.538579	−1.711583	4.3276
11.2507	−2.535825	−1.709174	4.2918
11.2533	−2.534562	−1.708229	4.2699
11.2448	−2.533872	−1.712866	4.1717
11.2358	−2.535293	−1.717807	4.1451
11.2227	−2.537565	−1.725049	4.1158
11.2152	−2.538937	−1.729381	4.1013
11.2076	−2.540360	−1.733373	4.0876
11.1627	−2.549029	−1.757150	4.0195
10.9984	−2.583200	−1.819053	3.8566
10.5602	−2.677624	−1.907134	3.6479
10.1071	−2.764945	−1.958555	3.5408
9.7737	−2.816340	−1.980309	3.5057
9.5627	−2.843675	−1.988750	3.5110
9.4022	−2.863435	−1.990593	3.5487

$\gamma = -9/11$ (f, g-symmetries);

Figures 11 and 13, Curve A.

* These orbits have the f-symmetry.

** These values have been calculated from the results of Shearing (2).

15.231	1.247	1.102	**
14.724	1.292	1.132	**
14.224	1.342	1.164	**
13.699	1.400	1.200	**
12.922	1.476	1.255	**
12.644	1.483	1.274	**
12.499	1.477	1.283	**
12.311	1.454	1.293	**
12.181	1.426	1.297	**
11.920	1.340	1.288	**
11.724	1.258	1.261	**
11.605	1.207	1.239	**
11.376	1.116	1.191	**

T	E_i	F_f	x
11.100	1.019	1.130	**
10.683	0.892	1.036	**
10.2900	0.788296	0.950629	1.0332
9.2903	0.564156	0.733819	1.0753
8.2903	0.371976	0.511284	1.1449
7.2903	0.196004	0.270076	1.2411
6.2904	0.023770	0.002084	1.3547
5.5100	−0.118624	−0.205141	1.4242
4.6337	−0.290232	−0.408913	1.4624
3.7583	−0.473530	−0.589031	1.4720
2.8783	−0.675276	−0.762007	1.4657
1.9983	−0.911227	−0.942263	1.4495
1.5583	−1.056078	−1.043772	1.4384
1.1183	−1.246079	−1.165971	1.4246
1.0194	−1.303097	−1.200864	1.4210
0.9794	−1.329290	−1.216425	1.4194
0.7896	−1.540585	−1.332620	1.4088
0.7820	−1.683283	−1.404321	1.4054
0.8020	−1.703969	−1.414107	1.4046
0.8820	−1.783020	−1.450669	1.4034
0.9600	−1.840791	−1.476362	1.4032
1.0000	−1.865086	−1.486907	1.4033
1.4600	−2.051660	−1.564047	1.4076
2.0713	−2.197426	−1.624702	1.4167
2.8233	−2.313029	−1.675323	1.4302
3.7033	−2.400549	−1.721602	1.4493
4.5833	−2.456050	−1.758555	1.4725
5.4633	−2.488933	−1.789498	1.5010
6.3433	−2.503861	−1.809594	1.5358
6.7833	−2.505109	−1.817321	1.5560
7.2233	−2.502276	−1.823638	1.5783
8.1033	−2.484110	−1.825384	1.6296
8.9833	−2.448882	−1.816871	1.6912
9.8633	−2.397534	−1.792868	1.7655
10.7433	−2.333755	−1.747897	1.8604
11.7833	−2.249944	−1.644238	2.0472
11.9833	−2.233641	−1.611882	2.1124
12.1833	−2.217989	−1.567557	2.2139*
12.2033	−2.216543	−1.561602	2.2289*
12.2761	−2.212028	−1.533330	2.3081*
12.2721	−2.218049	−1.494252	2.4655*
12.1943	−2.229360	−1.487093	2.5462*
11.8006	−2.277809	−1.526302	2.7056*
11.5029	−2.305139	−1.451825	2.6132*
10.8902	−2.363811	−1.290298	2.4792*
10.0190	−2.448350	−1.097752	2.3899*
9.2626	−2.517487	−0.936826	2.3512*
8.4145	−2.584999	−0.750859	2.3360*
7.6180	−2.635563	−0.561239	2.3494*
6.7970	−2.674465	−0.338695	2.3976*
6.0142	−2.698961	−0.088317	2.4789*
5.2255	−2.707236	0.172146	2.5545*
4.4991	−2.699903	0.367719	2.5777*
3.6040	−2.676902	0.564208	2.5694*
2.8614	−2.646401	0.710664	2.5491*
2.1401	−2.603337	0.848818	2.5240*
1.5920	−2.557019	0.955272	2.5028*
1.0866	−2.497265	1.057548	2.4821*
0.5459	−2.401224	1.175888	2.4587*
0.1575	−2.292371	1.272361	2.4411*
−0.1516	−2.149574	1.365939	2.4267*
−0.3227	−2.001001	1.440968	2.4187*
−0.3934	−1.864596	1.498470	2.4174*
−0.3222	−1.692910	1.550766	2.4185*
−0.1773	−1.547242	1.586427	2.4243*
+0.0636	−1.398123	1.614729	2.4333*
0.4639	−1.222441	1.640238	2.4471*
0.8684	−1.082288	1.658848	2.4603*
1.4761	−0.905601	1.679616	2.4799*
2.0831	−0.751666	1.699475	2.5003*
2.7969	−0.586967	1.721554	2.5271*
3.3554	−0.465582	1.740442	2.5509*

$\gamma = -0.59$ (g-symmetry); Figure 4, Curve g.

14.0391	1.335470	−1.146839	2.4200
13.4391	1.357690	−1.185442	2.6763
13.0391	1.332525	−1.232692	2.8132
12.6391	1.239741	−1.297538	2.9005
12.4391	1.153394	−1.316543	2.9219
12.2391	1.054082	−1.306192	2.9251
12.0391	0.963654	−1.276186	2.9218
11.6391	0.818161	−1.200468	2.9250
11.0391	0.651431	−1.082168	2.9637
10.2400	0.475674	−0.923333	3.0667
9.4400	0.327879	−0.755418	3.2263
8.6407	0.199480	−0.562915	3.4646
7.8407	0.094959	−0.287204	3.8942

$\gamma = +9/11$ (g-symmetry);
Figures 11, 12, 13 and 14, Curve C.

14.0390	0.680781	0.636390	0.9959
13.7938	0.718637	0.654282	1.0692
13.6147	0.767817	0.649758	1.1459
13.5816	0.808744	0.616295	1.1837
13.5596	0.964421	0.436785	1.3973
13.5241	1.050644	0.274133	1.8272
13.4968	1.055114	0.224883	1.9594

T	E_i	F_f	x
13.4395	1.050268	0.164973	2.0808
13.1871	1.015602	0.023768	2.2442
12.5729	0.935369	– 0.175966	2.3762
11.9284	0.847377	– 0.335339	2.4754
11.2869	0.744659	– 0.477699	2.5780
10.7105	0.624155	– 0.591546	2.6844
10.5084	0.564759	– 0.617667	2.7313
10.4067	0.521683	– 0.616135	2.7655
10.3621	0.459897	– 0.563973	2.8228
10.3802	0.442555	– 0.533356	2.8428
10.4821	0.404790	– 0.422874	2.8940
10.5855	0.367760	– 0.202000	2.9022
10.6065	0.368688	– 0.150906	2.9016
10.6656	0.407624	0.051942	2.8827
10.6407	0.417179	0.080296	2.8554
10.5814	0.439198	0.129813	2.7818
10.5494	0.478806	0.193241	2.6679
10.5835	0.510166	0.236258	2.5933
10.7910	0.582645	0.330997	2.4397
10.984	0.627	0.390	**
11.343	0.692	0.483	**
11.647	0.738	0.552	**
11.818	0.758	0.588	**
12.198	0.797	0.663	**
12.439	0.813	0.704	**
12.773	0.818	0.744	**
13.003	0.798	0.755	**
13.273	0.736	0.765	**
13.299	0.703	0.789	**
13.290	0.674	0.816	**
13.221	0.602	0.893	**
13.157	0.536	0.960	**
13.102	0.435	1.021	**
13.057	0.351	1.024	**
12.9290	0.222635	0.988521	1.7748
12.6791	0.075572	0.922258	1.8436
12.3791	– 0.053539	0.850330	1.9093
11.7791	– 0.260750	0.710125	2.0558
11.1791	– 0.440190	0.558572	2.2419
10.6262	– 0.584987	0.390094	2.4674
10.4919	– 0.611756	0.338073	2.5372
10.3912	– 0.624059	0.289597	2.6012
10.3092	– 0.613173	0.223513	2.6867
10.3005	– 0.595249	0.193677	2.7249
10.3498	– 0.530704	0.129750	2.8057
10.4875	– 0.423678	0.022423	2.8997
10.4969	– 0.407107	– 0.018082	2.9117
10.4848	– 0.401482	– 0.058964	2.9158
10.4718	– 0.401617	– 0.081997	2.9161

T	E_i	F_f	x
10.4563	– 0.403193	– 0.105263	2.9157
10.4022	– 0.415266	– 0.182693	2.9149
10.3597	– 0.439598	– 0.315852	2.9312
10.2600	– 0.515736	– 0.476393	2.9449
10.0600	– 0.652283	– 0.641896	2.9306
9.9114	– 0.807275	– 0.799587	2.9171
9.8971	– 0.840753	– 0.831121	2.9154
9.9087	– 0.940753	– 0.918336	2.9108
10.0027	– 1.023544	– 0.980197	2.9022
10.1023	– 1.072767	– 1.013361	2.8906
10.4920	– 1.150471	– 1.074153	2.8335
10.7997	– 1.175403	– 1.108956	2.7913
11.0705	– 1.186218	– 1.132634	2.7627
11.5005	– 1.194132	– 1.159512	2.7372
11.9400	– 1.196570	– 1.175956	2.7436
12.3341	– 1.195946	– 1.181945	2.7964

$\gamma = 9/11$ (g-symmetry);
Figures 12 and 14, Curve G.

T	E_i	F_f	x
0.7156	– 3.700695	1.859799	1.6389
0.5407	– 3.750055	1.908867	1.6476
0.3864	– 3.802089	1.965810	1.6661
0.3448	– 3.827983	2.005692	1.6845
0.3878	– 3.846018	2.058145	1.7169
0.5574	– 3.845713	2.114023	1.7660
0.8771	– 3.831725	2.179055	1.8566
0.9780	– 3.834734	2.204000	1.9088
0.9962	– 3.845484	2.217969	1.9449
0.8962	– 3.888893	2.239284	2.0129
0.5176	– 3.988867	2.257995	2.0944
– 0.0634	– 4.125582	2.265812	2.1593
– 1.2349	– 4.399732	2.250217	2.2189
– 2.4007	– 4.698202	2.201299	2.2239
– 3.5145	– 5.007979	2.107994	2.1600
– 4.2576	– 5.191019	1.971236	2.0604
– 4.4522	– 5.214952	1.901894	2.0272
– 4.5687	– 5.213574	1.840010	2.0071
– 4.7570	– 5.153683	1.655350	1.9896
– 4.7715	– 5.157711	1.653026	1.9904
– 4.6697	– 5.049989	1.534402	1.9935
– 4.5337	– 4.939664	1.396562	2.0148
– 4.2170	– 4.774818	1.196553	2.0634
– 3.2087	– 4.427356	0.807624	2.1982
– 2.1086	– 4.142273	0.603127	2.2916
– 1.0368	– 3.903481	0.491126	2.3489
0.0587	– 3.681083	0.401402	2.3740
1.0332	– 3.496193	0.328849	2.3374
2.0038	– 3.319443	0.284897	2.2613
3.1895	– 3.101219	0.263050	2.1985

T	E_i	F_f	x
4.1832	−2.908996	0.256105	2.1769
5.1776	−2.699075	0.255187	2.1811
6.1696	−2.455339	0.260133	2.2155
6.9315	−2.216746	0.270120	2.2732
7.2713	−2.080012	0.278048	2.3145
7.5731	−1.928359	0.288797	2.3654
7.8329	−1.763236	0.303189	2.4252
8.0041	−1.635239	0.316974	2.4737
8.1925	−1.484763	0.337991	2.5312
8.3075	−1.393569	0.355377	2.5651
8.4010	−1.321877	0.374375	2.5908
8.4979	−1.251594	0.405401	2.6145
8.5447	−1.220041	0.441797	2.6243
8.5480	−1.218381	0.449797	2.6247
8.5440	−1.222691	0.477079	2.6222
8.5063	−1.251865	0.517992	2.6098
8.4001	−1.335671	0.581846	2.5744
8.3181	−1.403528	0.620847	2.5442
8.1283	−1.566627	0.700280	2.4671
7.9730	−1.697961	0.758427	2.4021
7.8095	−1.822623	0.814228	2.3383
7.4112	−2.059182	0.930305	2.2105
6.9589	−2.251186	1.038466	2.0993
6.0707	−2.529227	1.206177	1.9394
5.0521	−2.781022	1.354541	1.8154
3.9467	−3.020587	1.486730	1.7260
2.9609	−3.222303	1.592559	1.6737
1.9717	−3.424375	1.699411	1.6415
1.0836	−3.616442	1.814117	1.6324
0.9147	−3.657125	1.845413	1.6342

$\gamma = 0.93$ (g-symmetry);
Figures 12 and 14, Curve D.

T	F_i	E_f	x
13.2240	−0.488930	0.503092	1.1430
13.0051	−0.514832	0.533287	1.2324
12.8323	−0.537660	0.562478	1.3234
12.7000	−0.555573	0.589866	1.4120
12.6299	−0.562315	0.609292	1.4696
12.6133	−0.564438	0.613521	1.4843
12.5542	−0.556286	0.644876	1.5508
12.5062	−0.382150	0.812581	1.8571
12.4915	−0.301807	0.869917	2.1548
12.4117	−0.118597	0.884336	2.8321
12.3332	−0.047234	0.864601	2.9465
12.2332	0.020154	0.840716	3.0239
12.1252	0.080000	0.815771	3.0846
11.7666	0.240000	0.732949	3.2450
11.3454	0.400000	0.631707	3.4122
11.0672	0.500000	0.544044	3.5358
10.5800	0.627164	0.354872	3.6536
10.4200	0.626307	0.286414	3.5822
10.2146	0.645000	0.238136	3.4487
10.0675	0.680000	0.220593	3.3584
9.1164	0.980000	0.186426	2.8393
8.0000	1.177707	0.177816	2.4596
7.1260	1.260000	0.179116	2.2845
6.0000	1.320350	0.185273	2.1373
5.0000	1.345946	0.191669	2.0504
4.0000	1.351175	0.200192	1.9904
3.0000	1.338000	0.207716	1.9517
2.0000	1.305000	0.232937	1.9244
1.0000	1.250000	0.249836	1.9175
0.0000	1.165000	0.277808	1.9266
−0.5000	1.109000	0.278941	1.9456
−1.0000	1.038004	0.300404	1.9656
−1.5000	0.949885	0.324630	1.9965
−2.0000	0.840000	0.351809	2.0435
−2.5000	0.701000	0.376278	2.1209
−2.8343	0.555000	0.368448	2.2409
−2.8485	0.500000	0.353191	2.3005
−2.7678	0.450000	0.329243	2.3646
−2.5523	0.400000	0.302053	2.4372
−2.1363	0.350000	0.284884	2.5143
−1.5500	0.307310	0.251536	2.5938
−1.0000	0.278582	0.218663	2.6632
−0.5000	0.257659	0.225769	2.6686
0.0000	0.239626	0.214755	2.6827
1.0000	0.211220	0.200992	2.6735
2.0000	0.191908	0.189724	2.6440
3.0000	0.179350	0.234175	2.6052
4.0000	0.170527	0.173423	2.6192
5.0000	0.164800	0.266115	2.6110
6.0000	0.160300	0.173615	2.6771
7.0000	0.157200	0.165522	2.7485
8.0000	0.154200	0.192022	2.8500
9.0956	0.144000	0.166225	3.0391
9.7113	0.120000	0.181916	3.1930
10.0705	0.080000	0.202184	3.3094
10.1750	0.060000	0.212549	3.3473
10.2574	0.040000	0.223548	3.3783
10.3820	0.000000	0.243160	3.4258
10.4745	−0.040000	0.266229	3.4575
10.6125	−0.120000	0.315446	3.4809
10.7444	−0.200000	0.379428	3.4176
10.9046	−0.280000	0.441285	3.2983
11.0000	−0.321000	0.474075	3.2195
11.1000	−0.360600	0.510672	3.1367

T	F_i	E_f	x
11.3000	– 0.433000	0.563644	2.9678
11.5000	– 0.498194	0.608467	2.7969
11.9000	– 0.606910	0.675444	2.4095
12.0000	– 0.626788	0.682825	2.2870
12.1000	– 0.640451	0.683870	2.1474
12.2000	– 0.645577	0.675182	1.9923
12.3000	– 0.642226	0.655647	1.8346
12.4000	– 0.642134	0.619104	1.6870
12.4165	– 0.650000	0.603747	1.6613
12.4221	– 0.660000	0.590363	1.6502
12.4129	– 0.700000	0.548753	1.6540
12.3851	– 0.750000	0.501709	1.7013
12.3558	– 0.798287	0.455343	1.7887
12.3344	– 0.838601	0.410235	1.9132
12.3130	– 0.875920	0.337678	2.1639
12.2906	– 0.877506	0.271212	2.3427
12.2711	– 0.870056	0.233220	2.4091
12.2524	– 0.862022	0.204344	2.4475
12.2336	– 0.853902	0.179472	2.4751
12.2086	– 0.843401	0.150700	2.5028
12.1126	– 0.805893	0.063070	2.5742
11.8355	– 0.708468	– 0.115447	2.7279
11.6699	– 0.652021	– 0.202378	2.8237
11.3220	– 0.527261	– 0.366831	3.0575
11.0181	– 0.404469	– 0.499704	3.3028
10.7419	– 0.272780	– 0.605993	3.5376
10.5339	– 0.147886	– 0.656723	3.6535
10.4497	– 0.093638	– 0.672478	3.6542
10.3476	– 0.039738	– 0.705331	3.6247
10.1254	0.030412	– 0.828737	3.5284
9.8214	0.074560	– 1.066666	3.3520
9.5836	0.089643	– 1.258016	3.1867
9.3141	0.100860	– 1.436682	3.0211
9.0266	0.108774	– 1.588898	2.8837
8.5251	0.117799	– 1.798625	2.7125
8.0253	0.122862	– 1.967355	2.5949
7.4471	0.127516	– 2.133586	2.4971
6.9718	0.130575	– 2.255053	2.4374
5.9881	0.136126	– 2.478703	2.3548
5.0067	0.142349	– 2.678135	2.3084
4.0180	0.150141	– 2.864845	2.2903
3.0244	0.159735	– 3.044130	2.2985
2.1264	0.170858	– 3.202577	2.3292
1.1272	0.187573	– 3.378280	2.3920
– 0.0670	0.219141	– 3.593373	2.4981
– 1.0555	0.255729	– 3.782701	2.5631
– 2.0395	0.295531	– 3.987019	2.5801
– 3.0164	0.347904	– 4.212430	2.5671
– 3.9786	0.453398	– 4.470982	2.5247

T	F_i	E_f	x
– 4.5419	0.614520	– 4.652011	2.4615
– 5.0795	0.898250	– 4.866938	2.3640
– 5.4109	1.097059	– 5.042387	2.3123
– 5.7004	1.293431	– 5.270761	2.2821
– 5.9020	1.499987	– 5.599470	2.2825
– 4.4236	2.152824	– 5.432072	2.6726
– 4.0368	2.185435	– 5.260352	2.7085
– 3.6467	2.212470	– 5.105056	2.7221
– 3.0584	2.245670	– 4.894431	2.7162
– 2.6654	2.263865	– 4.767325	2.7017
– 2.2720	2.279280	– 4.648491	2.6819
– 1.8788	2.292056	– 4.537502	2.6589
– 1.4858	2.302190	– 4.432771	2.6338
– 1.0932	2.309583	– 4.334424	2.6074
– 0.5003	2.315266	– 4.195032	2.5654
0.0910	2.314538	– 4.064088	2.5219
1.0818	2.302644	– 3.855107	2.4534
2.0751	2.282270	– 3.655248	2.3983
3.0694	2.255115	– 3.459504	2.3566
4.0603	2.220425	– 3.264416	2.3238
5.0466	2.175569	– 3.063928	2.2928
6.0205	2.114763	– 2.850004	2.2521
6.5630	2.067331	– 2.716241	2.2153
7.0597	2.000185	– 2.570271	2.1490
7.2788	1.945506	– 2.484930	2.0915
7.7594	1.726619	– 2.253396	2.0374
8.1699	1.597879	– 2.099951	2.1383
8.4641	1.504404	– 1.984724	2.2441
8.6881	1.430120	– 1.890738	2.3460
9.0871	1.277921	– 1.697697	2.5899
9.2802	1.191095	– 1.586235	2.7468
9.7399	0.948418	– 1.240496	3.2389
10.0020	0.825556	– 1.005077	3.5327
10.1021	0.796474	– 0.930571	3.6313
10.2028	0.784632	– 0.875752	3.7291
10.3328	0.806889	– 0.852516	3.8613
10.4915	0.857416	– 0.886197	3.9671
10.7917	0.910092	– 0.956138	3.9228
11.0193	0.942125	– 0.982870	3.8376
11.3698	0.979447	– 1.001444	3.7504
11.7544	1.001275	– 1.009391	3.7652
12.1722	1.003396	– 1.010790	4.3598

F = 0.0 (ejection, g-symmetry);
Figure 1, Curves E and F.

T	γ	E_f	x
5.3514	– 0.999639	0.000012	1.2943
5.9513	– 0.883473	0.014317	1.3324

T	γ	E_f	x
6.5512	−0.764800	0.029161	1.3755
7.4512	−0.581461	0.052562	1.4522
8.3512	−0.391225	0.077855	1.5496
9.2512	−0.194515	0.106713	1.6803
10.1509	0.000000	0.146644	1.8694
10.7498	0.098541	0.200964	2.0552
10.8988	0.108051	0.225672	2.1153
11.0488	0.103065	0.260803	2.1892
11.1988	0.062626	0.320117	2.3148
11.1410	0.006675	0.834330	2.4512
11.1010	0.029614	0.810811	2.3432
11.0610	0.037779	0.800958	2.2917
11.0210	0.041608	0.794889	2.2529
10.9810	0.042819	0.791140	2.2205
10.9410	0.042143	0.788864	2.1921
10.9010	0.039989	0.787896	2.1666
10.8010	0.029627	0.789876	2.1103
10.7010	0.013859	0.796899	2.0613
10.5811	0.010506	0.810650	2.0085
10.4011	−0.056292	0.842194	1.9370
10.3011	−0.086461	0.866083	1.8996
10.1811	−0.128436	0.903476	1.8552
9.9728	−0.262116	1.061196	1.7490

T	γ	E_f	x
9.9736	−0.273962	1.079129	1.7414
9.9964	−0.300939	1.123677	1.7246
10.0978	−0.337786	1.195686	1.7022
10.2978	−0.366461	1.269645	1.6829
10.4974	−0.379446	1.317964	1.6704
10.7974	−0.386012	1.369043	1.6553
11.0974	−0.383091	1.404737	1.6418
11.3974	−0.373227	1.430109	1.6282
11.8474	−0.347407	1.453956	1.6098
12.2974	−0.308769	1.465026	1.5917
12.7474	−0.256100	1.465084	1.5751
13.3468	−0.157326	1.449030	1.5584
13.7952	−0.048610	1.421721	1.5545
14.1738	0.100000	1.377884	1.5692
14.3459	0.250000	1.325009	1.6063
14.3614	0.300000	1.305250	1.6243
14.3370	0.390000	1.268434	1.6660
14.1985	0.510000	1.211943	1.7686
13.7271	0.690000	1.112385	1.9541
13.1767	0.810000	1.013702	2.2554
12.5487	0.900000	0.905050	2.6962
12.1000	0.945000	0.812895	3.2331
11.6854	0.975000	0.707411	4.1351
11.3097	0.993000	0.567693	6.2107

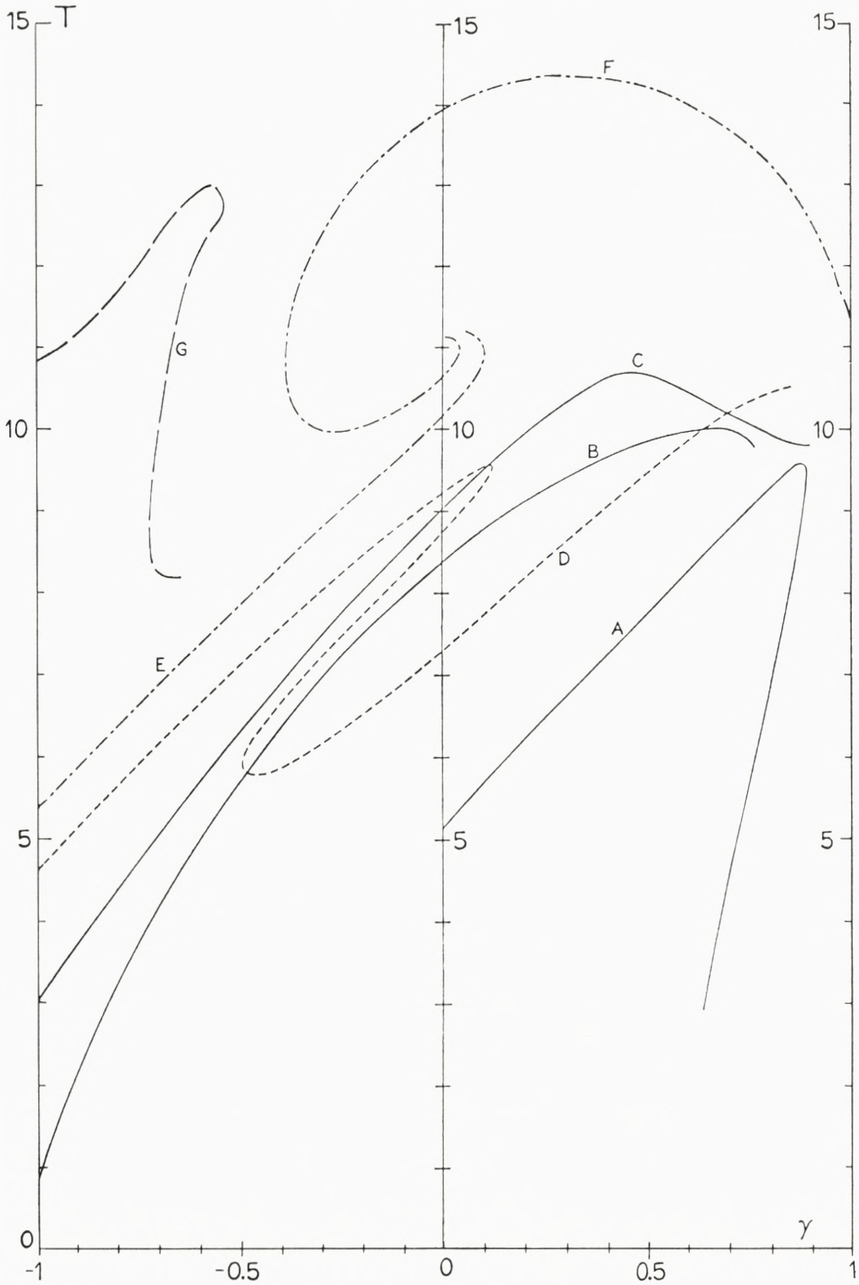

Figure 1: (T, γ) Profiles of Eigensurfaces.
(a) class: $F = 1.1$ (A); $F = 0.4$ (B); $F = 0.0$ (C); (n) class: $E = 0.0$ (D); (g) class: $F = 0.0$ (E), (F); $(\alpha\text{–}\delta)$ class: $F = -0.641489$ (G).

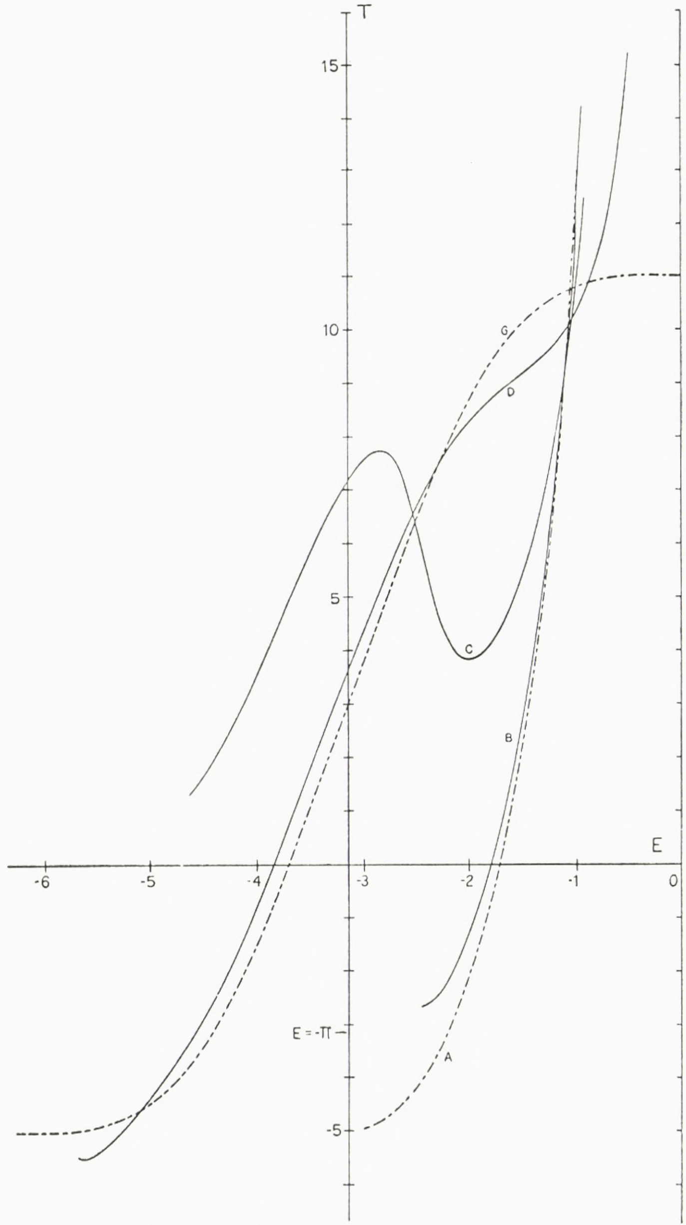

Figure 2: (T, E) Profiles for the (f) class.
$A\,(\gamma = -1)$; $B\,(\gamma = -9/11)$; $C\,(\gamma = 0)$; $D\,(\gamma = +9/11)$; $G\,(\gamma = +1$, using $n = 1)$.

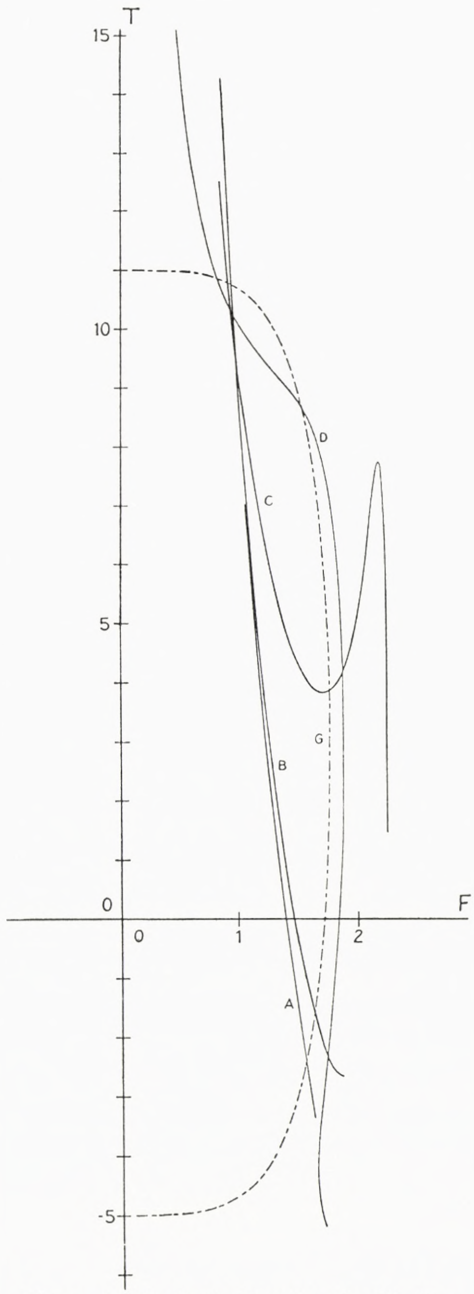

Figure 3: (T, F) Profiles for the (f) class.
$A(\gamma = -1)$; $B(\gamma = -9/11)$; $C(\gamma = 0)$; $D(\gamma = +9/11)$; $G(\gamma = +1$, using $n = 1)$.

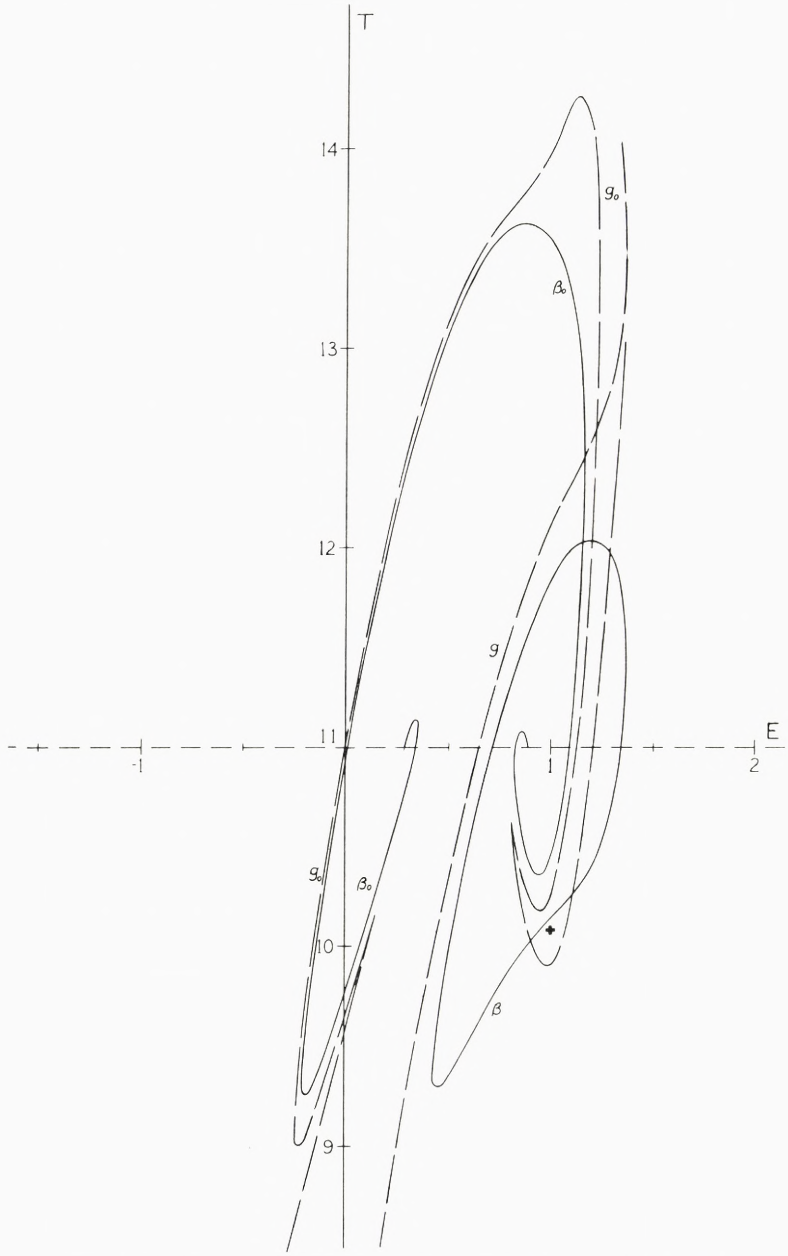

Figure 4: Detailed (T, E) Profiles for the (β) and (g) classes.
β, $g(\gamma = -0.59)$; β_0, g_0 $(\gamma = 0)$.
The heavy cross marks the approximate point of disappearance of the (β) class.

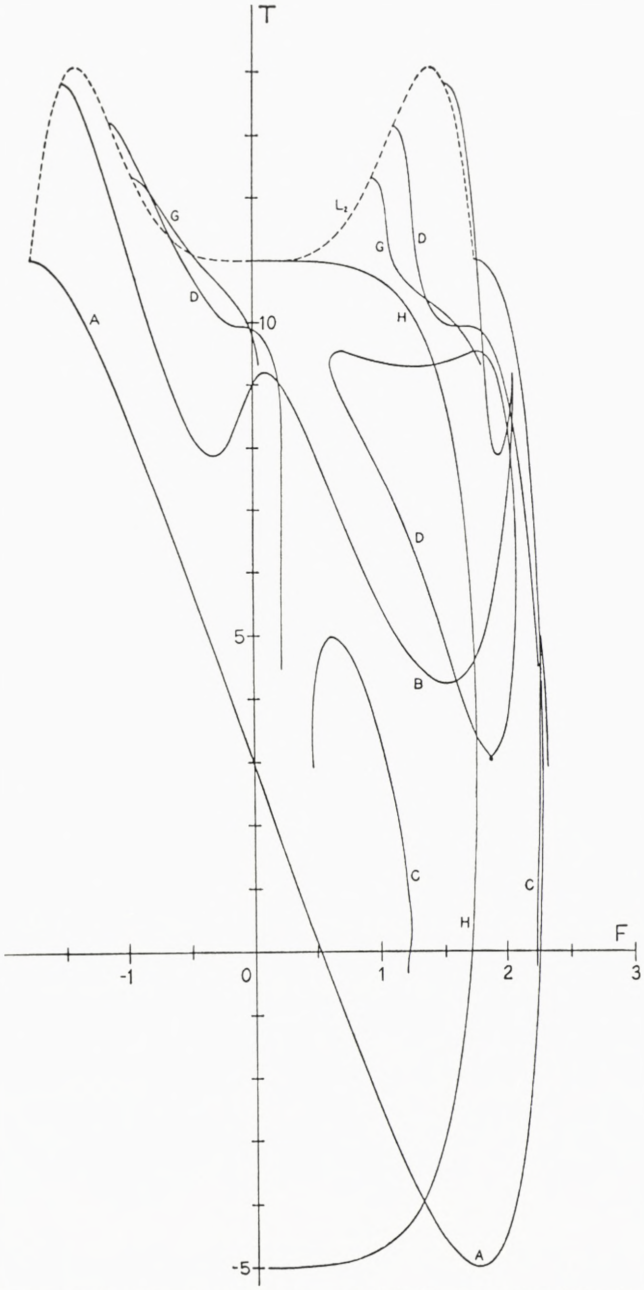

Figure 5: (T, F) Profiles for the (a) class, and (T, F) Locus for Libration Point L_2. $A(\gamma = -1$, using $n = 1)$; $B(\gamma = 0)$; $C(\gamma = 0.630199)$; $D(\gamma = +9/11$ for the upper portions of the bag, $\gamma = 0.8172$ and $\gamma = 0.81286$ for the "island" portion); $G(\gamma = 0.93)$; $H(\gamma = +1$, using $n = 1)$.

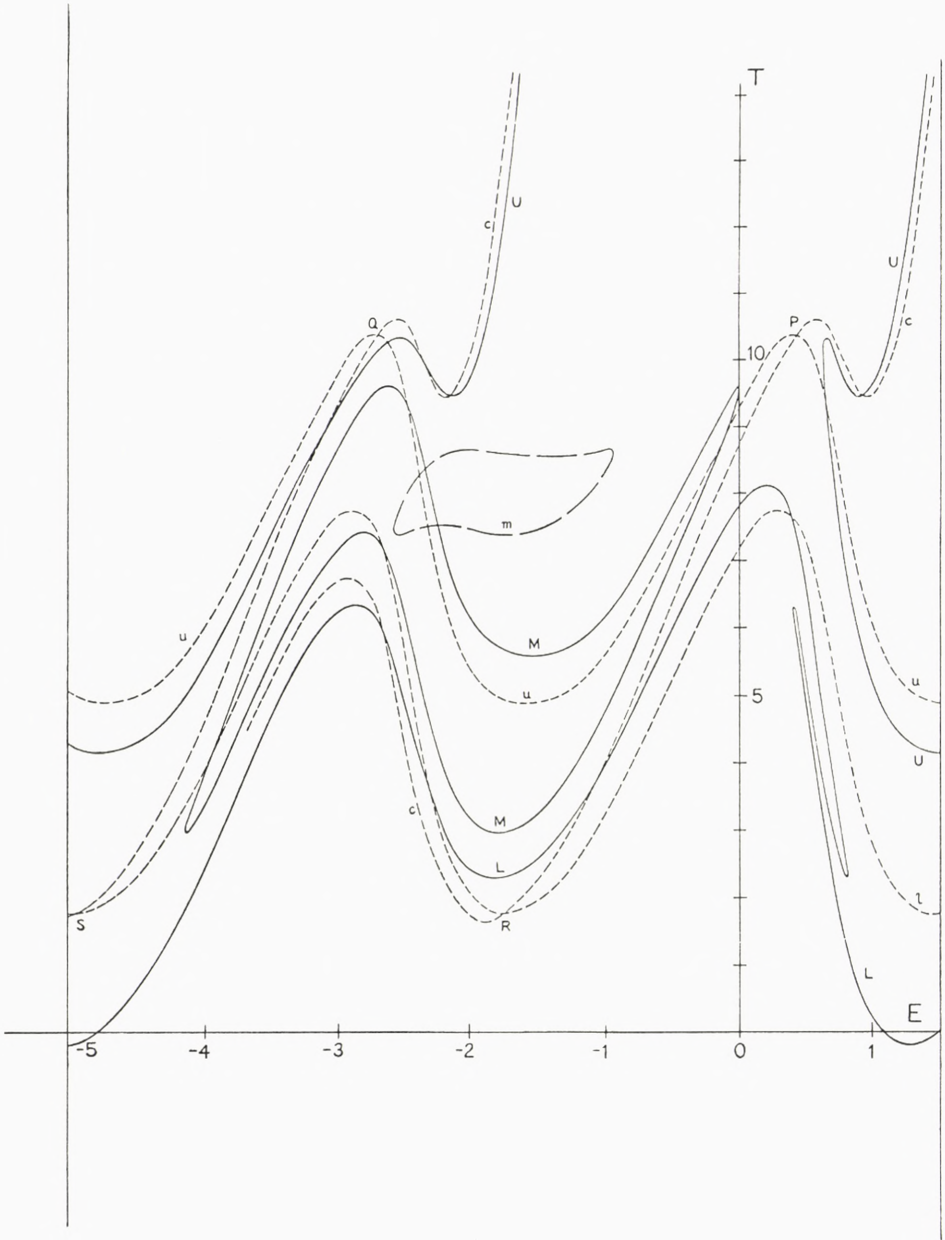

Figure 6: (T, E) Profiles for the (n) class.
u, c, l (upper, middle, lower branches at $\gamma = 0$); U, M, L (upper, middle, lower branches at $\gamma = 0.12$); m (middle branch at $\gamma = 0.664928$); P, Q, R, S are points referred to in the text.

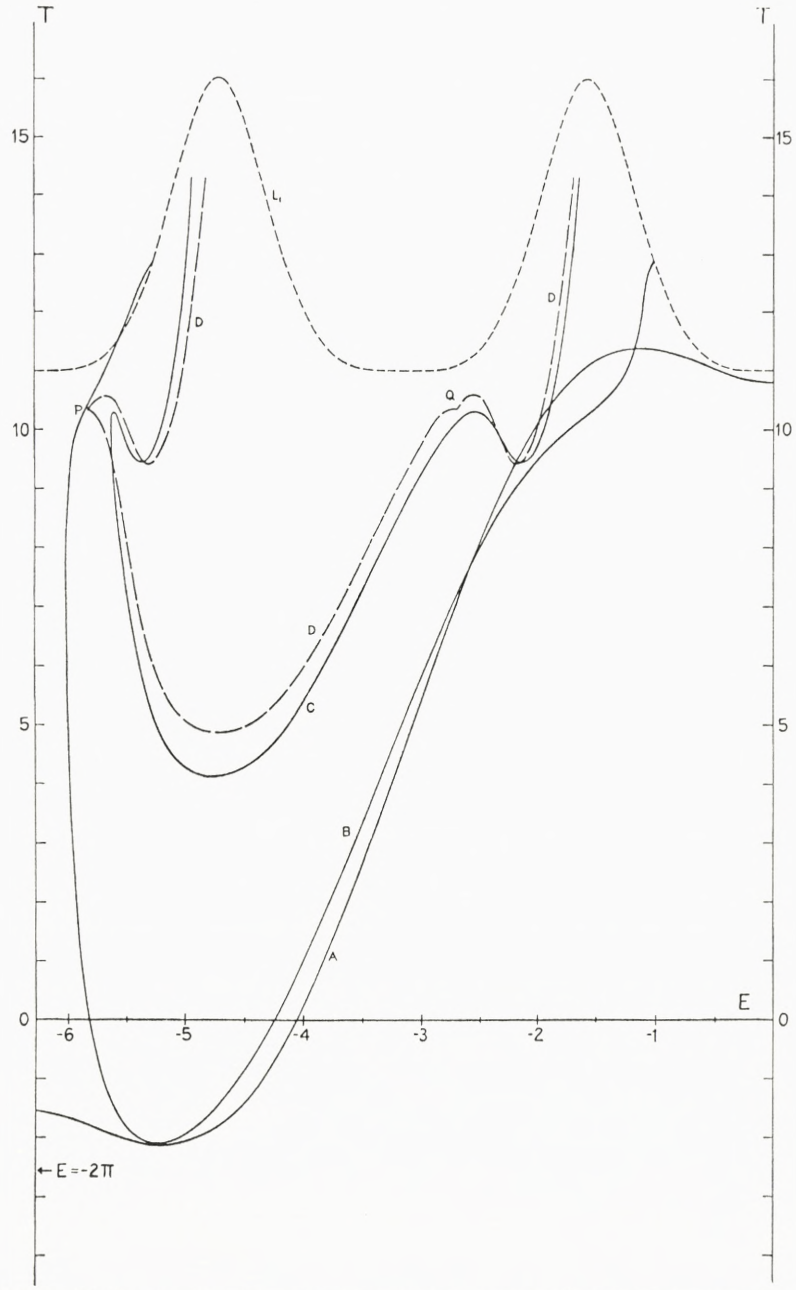

Figure 7: Detailed (T, E) Profiles for the Upper (n) class, and (T, E) Locus for Libration Point L_1. $A(\gamma = +1$, using $n = 5/3)$; $B(\gamma = 0.9)$; $C(\gamma = 0.12)$; $D(\gamma = 0$ composite of u and c branches); P, Q are points referred to in the text.

Figure 8: (T, F) Profiles for the $(\alpha\text{–}\delta)$ class, and associated zero velocity curves. $A(\gamma = -1,$ using $n = 3)$; $B(\gamma = -0.689294)$; $C(\gamma = 0)$; $D(\gamma = 0.8609)$; $P(\gamma = -0.545909)$; $S(\gamma = -0.709554)$; $V(\gamma = 0)$; a, b, c, d are corresponding zero velocity curves; e is the zero velocity curve for $\gamma = +1$.

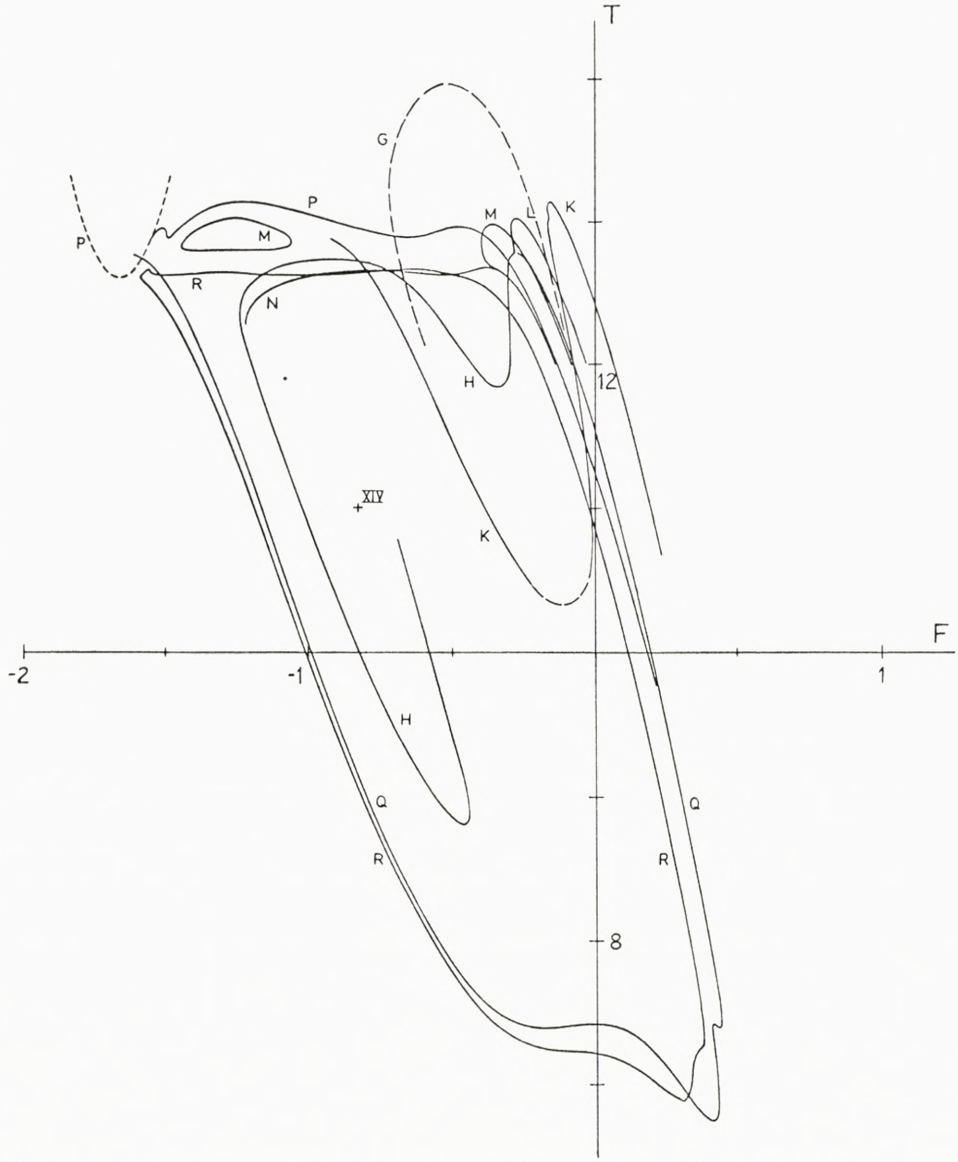

Figure 9: Detailed (T, F) Profiles for the $(\alpha\text{–}\delta)$ class, and associated zero velocity curves. $P(\gamma = -0.545909)$; $R(\gamma = -0.541909)$; $M, N(\gamma = -0.518320)$; $M(\gamma = -0.514645)$; $H, L, Q(\gamma = -0.483940)$; $K(\gamma = -0.402450)$; (δ) class profile: $G(\gamma = -0.402450)$; p is a corresponding zero velocity curve.

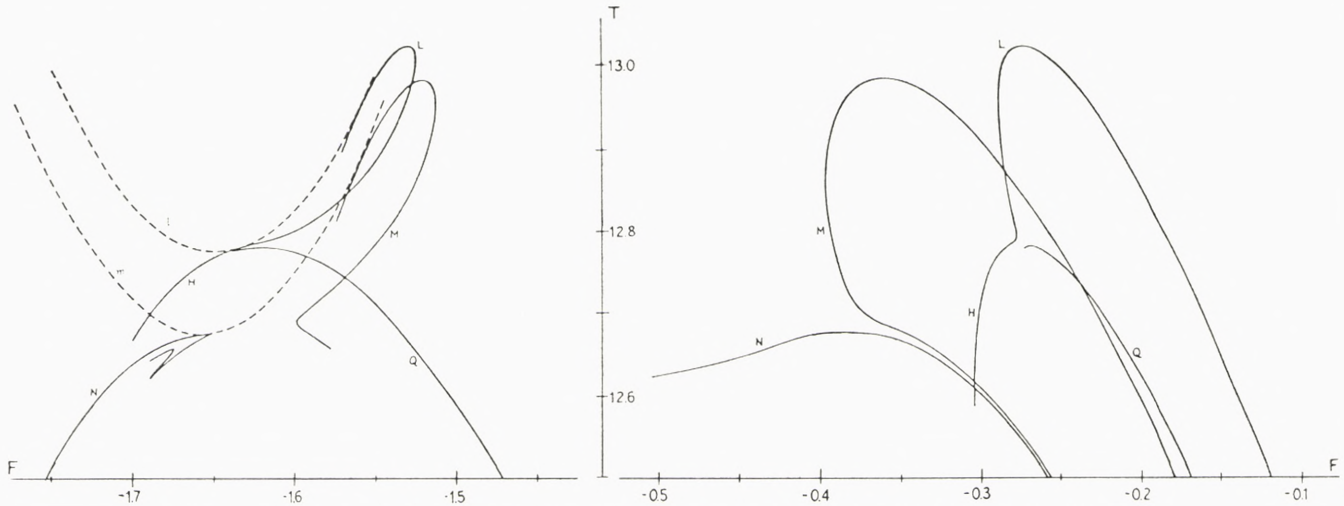

Figure 10: Detailed (T, F) Profiles for the $(\alpha\text{–}\delta)$ class, and associated zero velocity curves. M, N $(\gamma = -0.518320)$; H, L, Q $(\gamma = -0.483940)$; m, l are corresponding zero velocity curves. (α-type profiles on the left-hand side are mirror images of the usual profiles).

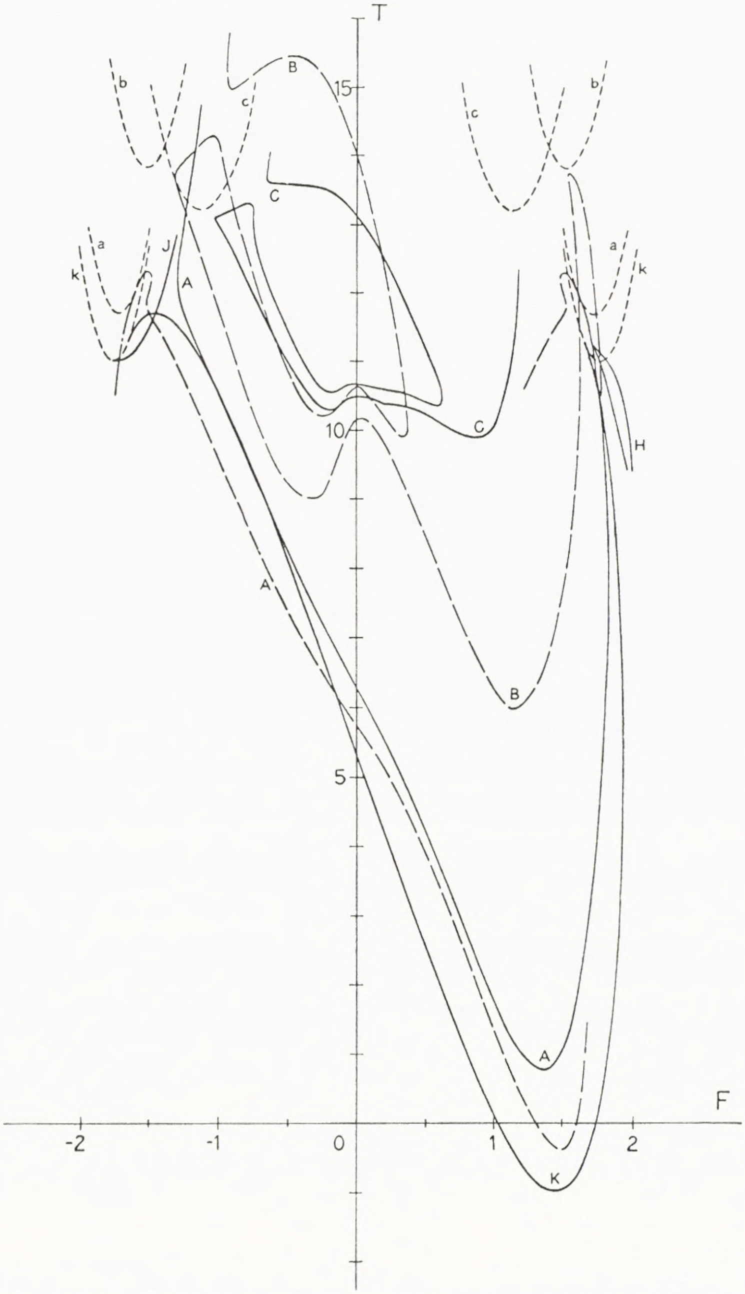

Figure 11: (T, F) Profiles for the (g) class, Evolution above $\gamma = -1$.
$A(\gamma = -9/11)$; $B(\gamma = 0)$; $C(\gamma = +9/11)$; $H(\gamma = -0.946809)$; $J(\gamma = -1$, using $e = 0)$; $K(\gamma = -1$, using $n = 2)$; a, b, c, k are corresponding zero velocity curves.

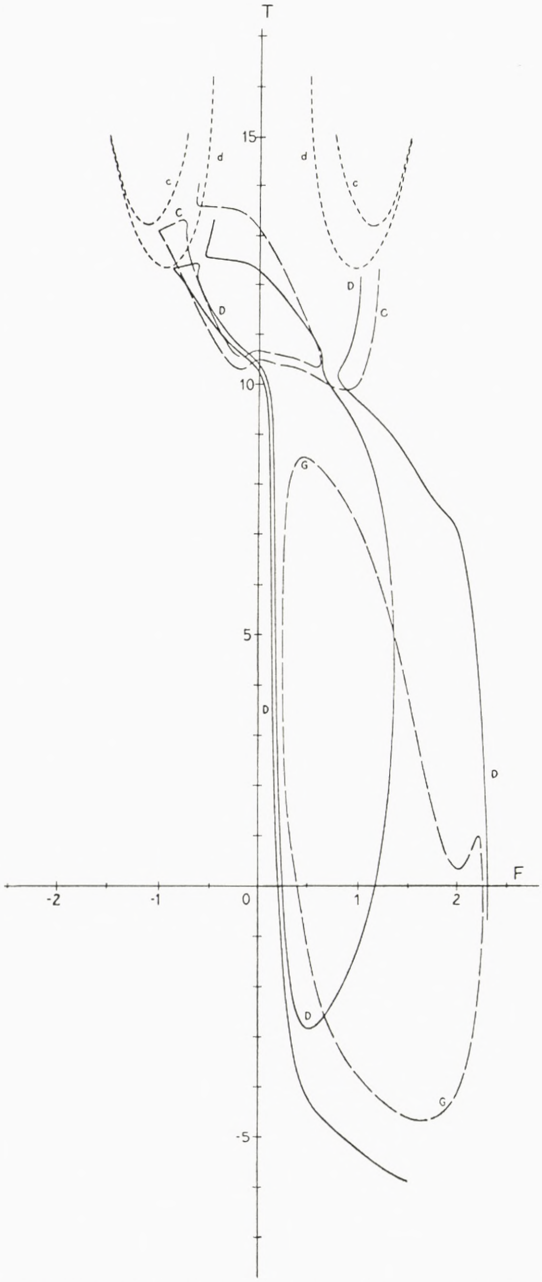

Figure 12: (T, F) Profiles for the (g) class, Evolution below $\gamma = +1$.
$C(\gamma = +9/11)$; $D(\gamma = 0.93)$; $G(\gamma = +9/11)$; c, d are corresponding zero velocity curves.

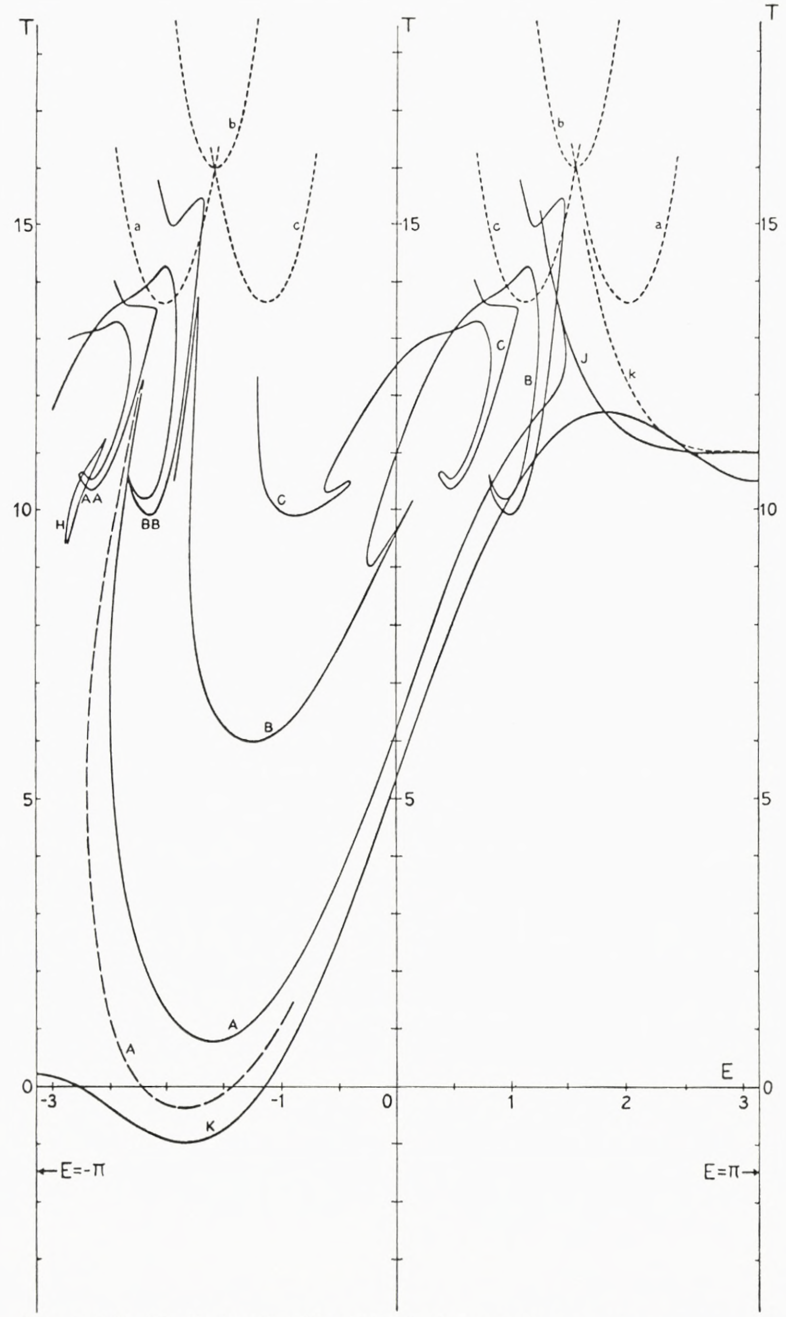

Figure 13: (T, E) Profiles for the (g) class, Evolution above $\gamma = -1$. A, $AA(\gamma = -9/11)$; B, $BB(\gamma = 0)$; $C(\gamma = +9/11)$; $H(\gamma = -0.946809)$; $J(\gamma = -1$, using $e = 0)$; $K(\gamma = -1$, using $n = 2)$; a, b, c, k are corresponding zero velocity curves.

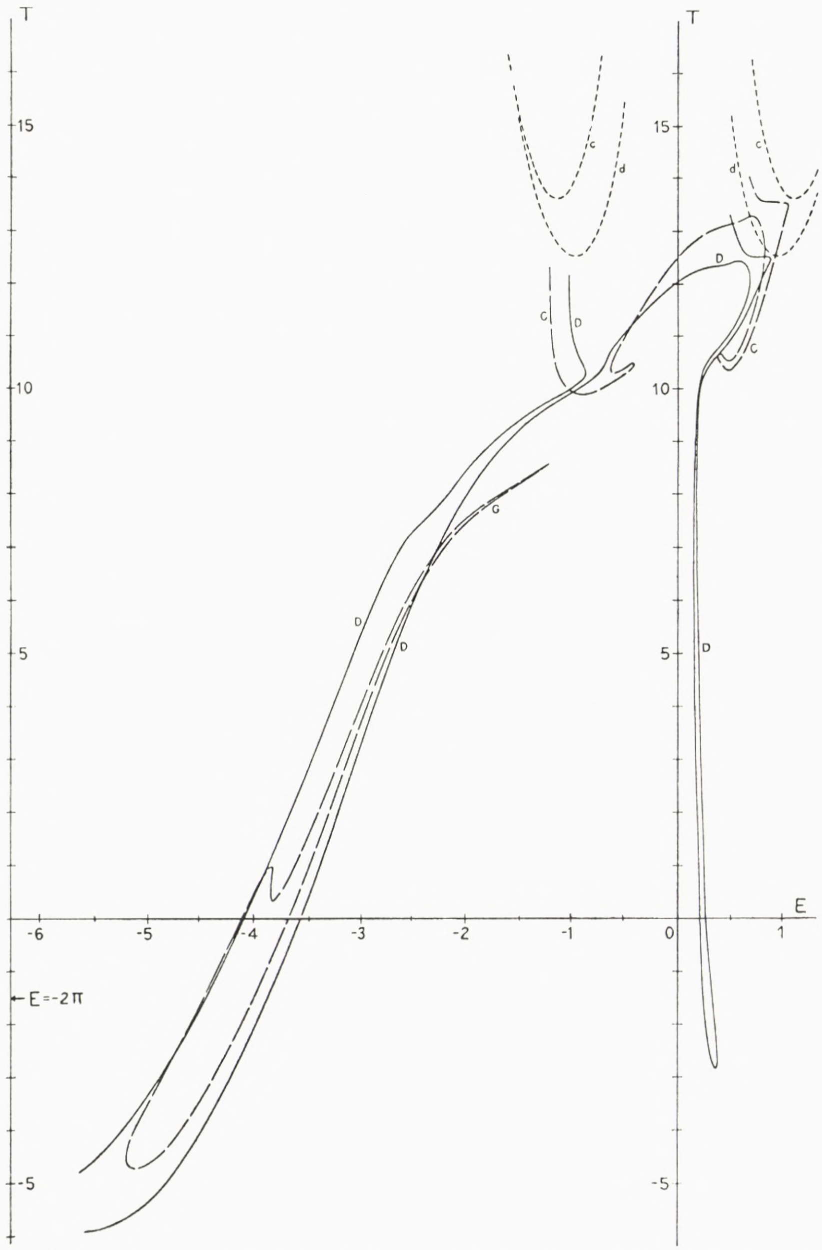

Figure 14: (T, E) Profiles for the (g) class, Evolution below $\gamma = +1$.
$C(\gamma = +9/11)$; $D(\gamma = 0.93)$; $G(\gamma = +9/11)$; c, d are corresponding zero velocity curves.

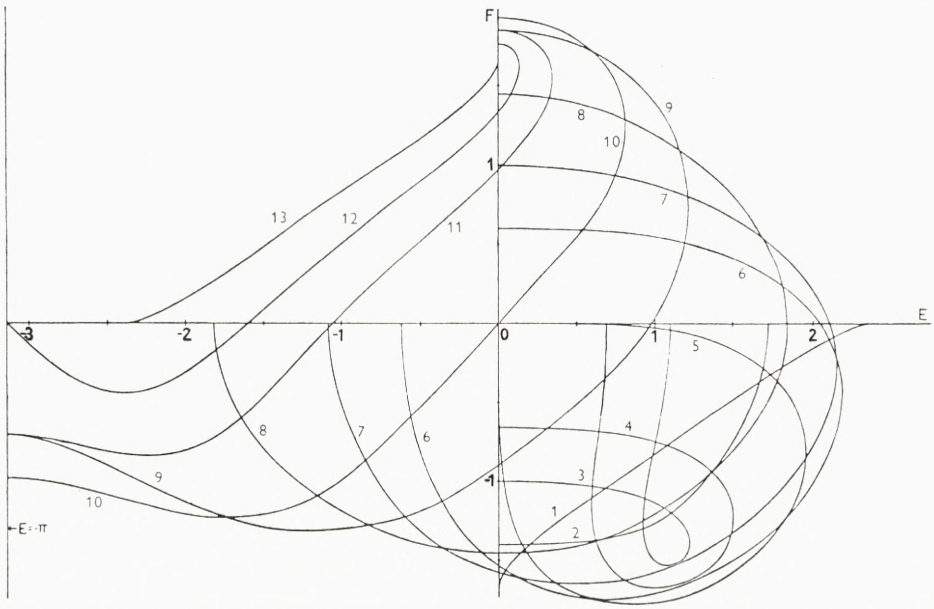

Figure 15: Development of the (g) class ($\gamma = -1$, $e \neq 0$, $n = 2$) for selected r and J values. (Limiting orbits 1 and 13 have $r = 1.719358$ and $J > 0$.)

Indleveret til Selskabet den 1. februar 1965.
Færdig fra trykkeriet den 13. august 1965.

Det Kongelige Danske Videnskabernes Selskab

Matematisk-fysiske Skrifter

Mat. Fys. Skr. Dan. Vid. Selsk.

Bind **1** (kr. 141,00)

kr. ø.

1. Brodersen, Svend, and Langseth, A.: The Infrared Spectra of Benzene, sym-Benzene-d_3, and Benzene-d_6. 1956 14,00
2. Nörlund, N. E.: Sur les fonctions hypergéométriques d'ordre supérieur. 1956 .. 15,00
3. Fröman, Per Olof: Alpha Decay of Deformed Nuclei. 1957 20,00
4. Brodersen, Svend: A Simplified Procedure for Calculating the Complete Harmonic Potential Function of a Molecule from the Vibrational Frequencies. 1957 10,00
5. Brodersen, Svend, and Langseth, A.: A Complete Rule for the Vibrational Frequencies of Certain Isotopic Molecules. 1958 6,00
6. Källén, G., and Wightman, A.: The Analytic Properties of the Vacuum Expectation Value of a Product of three Scalar Local Fields. 1958 15,00
7. Brodersen, Svend, and Langseth, A.: The Fundamental Frequencies of all the Deuterated Benzenes. Application of the Complete Isotopic Rule to New Experimental Data. 1959 10,00
8. Mottelson, Ben R., and Nilsson, Sven Gösta: The Intrinsic States of Odd-A Nuclei having Ellipsoidal Equilibrium Shape. 1959 22,00
9. Källén, G., and Wilhelmsson, H.: Generalized Singular Functions. 1959 6,00
10. Møller, C.: Conservation Laws and Absolute Parallelism in General Relativity. 1961 15,00
11. Soloviev, V. G.: Effect of Pairing Correlation on Energies and β-Transition Probabilities in Deformed Nuclei. 1961 8,00

Bind **2**

(*uafsluttet / in preparation*)

1. Higgins, Joseph: Theory of Irreversible Processes. I. Parameters of Smallness. 1962 17,00
2. Gallagher, C. J., Jr., and Soloviev, V. G.: Two-Quasi-Particle States in Even-Mass Nuclei with Deformed Equilibrium Shape. 1962 18,00
3. Mang, H. J., and Rasmussen, J. O.: Shell Model Calculations of Alpha Decay Rates of Even-Even Spheroidal Nuclei. 1962 12,00
4. Pellegrini, C., and Plebanski, J.: Tetrad Fields and Gravitational Fields. 1963 .. 14,00
5. Nörlund, N. E.: The Logarithmic Solutions of the Hypergeometric Equation. 1963 23,00
6. Lütken, Hans, and Winther, Aage: Coulomb Excitation in Deformed Nuclei. 1964 9,00
7. Bartlett, James H.: The Restricted Problem of Three Bodies. 1964 13,00
8. van Winter, Clasine: Theory of Finite Systems of Particles. I. The Green Function. 1964 20,00
9. Gyldenkerne, Kjeld: A Three-Dimensional Spectral Classification of G and K Stars. 1964 14,00
10. van Winter, Clasine: Theory of Finite Systems of Particles. II. Scattering Theory. (In preparation).

Bind **3**

(*uafsluttet / in preparation*)

1. Bartlett, J. H., and Wagner, C. A.: The Restricted Problem of Three Bodies (II). 1965 17,00

On direct application to the agent of the Academy, Ejnar Munksgaard, Publishers, 6 Nörregade, Köbenhavn K., a subscription may be taken out for the series *Matematisk-fysiske Skrifter*. This subscription automatically includes the *Matematisk-fysiske Meddelelser* in 8vo as well, since the *Meddelelser* and the *Skrifter* differ only in size, not in subject matter. Papers with large formulae, tables, plates etc., will as a rule be published in the *Skrifter*, in 4to.

For subscribers or others who wish to receive only those publications which deal with a single group of subjects, a special arrangement may be made with the agent of the Academy to obtain the published papers included under one or more of the following heads: *Mathematics, Physics, Chemistry, Astronomy, Geology.*

In order to simplify library cataloguing and reference work, these publications will appear without any special designation as to subject. On the cover of each, however, there will appear a list of the most recent paper dealing with the same subject.

The last published numbers of *Matematisk-fysiske Skrifter* within the group of **Astronomy** are the following:

Vol. **2**, nos. 7, 9. – Vol. **3**, no. 1.

Printed in Denmark
Bianco Lunos Bogtrykkeri A/S